Hydrogeological impact assessment by tunnelling at sites of high sensitivity

Estanislao Pujades [1], Enric Vázquez-Suñé [1], Laura Culí [1], Jesus Carrera [1], Alberto Ledesma [2], Anna Jurado [1].

[1] GHS, Institute of Environmental Assessment and Water Research (IDAEA), CSIC, Barcelona, Spain

[2] Dept. Geotechnical Engineering and Geosciences, Universitat Politècnica de Catalunya, UPC-BarcelonaTech, Barcelona, Spain

Corresponding author: Estanislao Pujades

Phone: +34 93 400 61 00

Fax: +34 93 204 59 04

e-mail: estanislao.pujades@gmail.com

Abstract

A tunnel for the High Speed Train (HST) was constructed in Barcelona with an Earth Pressure balance (EPB) Tunnel Boring Machine (TBM). The tunnel crosses Barcelona and passes under some famous landmarks such as the Sagrada Familia and the Casa Milà. Both monuments are UNESCO world heritage sites and a committee appointed by the UNESCO acted as external observers during the construction. Concerns about soil settlements and the hydrogeological impacts of the construction were raised. These concerns were addressed during the design stage to forestall any unexpected events. The methodology consisted of 1) characterising the geology in detail, 2) predicting the impacts caused in the aquifer, 3) predicting the soil displacements due to water table oscillations produced by the construction, and 4) monitoring the evolution of groundwater and soil settlements. The main estimated impact on groundwater was a moderate barrier effect. The barrier effect, the magnitude of which matched the predictions, was detected during construction. The monitoring of soil settlements revealed short and long term movements. The latter movements matched the analytical predictions of soil displacements caused by the groundwater oscillations.

This paper proposes a realistic procedure to estimate impacts on groundwater during tunnel construction with an EPB. Our methodology will considerably improve the construction of tunnels in urban areas.

Key words: Sagrada Familia, Tunnel Boring Machine, Barrier Effect, Underground Construction, Groundwater, UNESCO

1. Introduction

The High Speed Train (HST) “Madrid-Barcelona-France frontier” crosses Barcelona in a Southwest-Northeast direction (Figure 1). The stretch of the tunnel in Barcelona was dug using an Earth Pressure Balance (EPB) Tunnel Boring Machine (TBM). Although the tunnel does not pass under any building, it passes by the front of the Sagrada Familia Basilica (declared Unesco World Heritage Site in 2005) and Casa Milà (declared Unesco World Heritage Site in 1984; Figure 1). The construction of the Basilica commenced in 1882 and is ongoing. It was designed by the Modernist architect Antonio Gaudi and is the maximum tourist attraction of Barcelona, drawing thousands of sightseers every year. The proximity of the tunnel to the Sagrada Familia Basilica led to much controversy among politicians and citizens, who feared for its safety during the construction of the tunnel.

These fears were enhanced by accidents and/or incidents that occurred during the construction of the HST tunnel in Barcelona. In 2005, a tunnel to extend the underground line 5 collapsed during the construction stage, affecting numerous residents of the El Carmel neighbourhood (Cia and Blanchar, 2005; Melis, 2005). Fortunately, there were no victims. The tunnel collapsed mainly (in addition to other factors associated with the construction) because of the presence of an undetected fault zone (Jimenez and Senent, 2012). Subsequently, problems arose during the construction of other stretches of the HST line “Madrid-Barcelona-France frontier”, e.g. in the Bellvitge neighbourhood in the South of Barcelona. The tunnel was constructed by the cut and cover method and numerous sink-holes appeared during the excavation. These were caused by defects in the diaphragm walls and could have affected adjacent buildings (Pujades *et al.*, 2012a). During the drilling of the HST tunnel in Barcelona other high profile incidents occurred in other parts of the world,

deepening the concern about the construction. One well known incident was the collapse of the underground tunnel in Cologne in 2009 (Van Baars, 2011).

Because of these setbacks, representatives of the Basilica, neighbourhood associations and some politicians launched a campaign against the construction. As a result, the construction specifications were made stricter than usual in order to avoid accidents and minimize the impact of the construction around the Sagrada Familia. The impacts were anticipated, the initial project was modified to mitigate them and additional safety measures were adopted.

It was initially planned to construct the tunnel by the cut and cover method. This option was not considered because the impact on the groundwater would have been excessive since the diaphragm walls obstructed a large portion of the aquifer. The hydraulic head would have been altered by more than 3 m, which would have affected the capacity of the soil to support loads and would have caused soil movements (heave on the upgradient side of the tunnel and subsidence downgradient). In addition, the cut and cover method causes considerable disruption to the normal life of cities. The tunnel was therefore constructed by using an EPB. Two protection measures were adopted in the areas adjacent to the Sagrada Familia in order to mitigate the impact and risks of the construction. First, a wall of non-secant piles (BPW) was built to reduce the tunnelling settlements under the Sagrada Familia (Rodríguez and Blanco, 2012). Second, a shaft was excavated near the Basilica (Pujades *et al.*, 2014a). The aim of this shaft was to service the EPB in order to excavate the tunnel under the Sagrada Familia with the EPB under optimal conditions. All the potential impacts were considered and are described below.

The most significant hydrogeological impacts potentially caused by the construction of a tunnel in an aquifer are the barrier effect (s_B) and the drain effect (Vázquez-Suñè *et al.*, 2005). The barrier effect is caused by underground impervious structures located below the

water table. These structures reduce the effective transmissivity of the aquifer, leading to a rise in the water table upgradient and to a drop downgradient (Ricci *et al.*, 2007; Deveughèle and Zokimila, 2010). The barrier effect may entail geotechnical and/or environmental consequences and may affect pre-existing infrastructures (Custodio and Carrera, 1989; Marinos and Kavvadas, 1997; Tambara *et al.*, 2003; Paris *et al.*, 2010). The drain effect is caused by drainage tunnels which are designed to extract groundwater so as to avoid water loads. These tunnels cause a head drop that may have far-reaching environmental and geotechnical consequences (Li and Kagami, 1997; Chae *et al.*, 2008; Vicenzi *et al.*, 2009; Butscher, 2012). Both effects can be determined accurately prior to the construction numerically and analytically (Goodman *et al.*, 1965; Meiri, 1985; El Tani, 1999, 2003; Kolymbas and Wagner, 2007; Pujades et al., 2012b). If the predictions show that these impacts are not acceptable, the construction must be modified or corrective measures must be adopted, eg. Kusumoto et al. (2003) proposes solutions to minimise the barrier effect).

Other impacts when tunnelling with an EPB include those related to the excavation of shafts, which are used as maintenance, emergency and/or ventilation exits (Ni and Cheng, 2011). The dewatering needed to excavate deep shafts causes a drop in the head and modifies the groundwater behaviour and the water pressure distribution around the shaft. The impacts of the head drop are similar to those of the drain effect (settlements are the most feared impact). However, the head drop (and associated settlements) is punctual. Moreover, accidents such as siphoning or base heave events may cause large soil movements outside the enclosure, posing a risk to adjacent buildings (DGGT, 2012).

Finally, the most perceptible impacts when tunnelling with an EPB are the soil movements during the tunnel excavation. Movements can be divided into short and long term movements. Short term movements are caused mainly by 1) ground loss during the excavation, which redistributes the stress in the soil and results in a stress relief (Ercelebi et

al., 2011), 2) injection of grout and 3) pushes of the TBM over the soil to advance. Long term movements are observed after the excavation process and are associated with creep, stress redistribution, consolidation of the soil after drainage, and perhaps with soil consolidation resulting from groundwater changes due to the interaction between the tunnel and the aquifer (Ercelebi et al., 2011; barrier effect or drain effect).

The methodology to assess all the potential impacts summarised above consisted in:

1) Characterising the soil geologically and hydrogeologically.
2) Predicting numerically and analytically the magnitude of the potential impacts caused by the construction: water levels and long term settlements associated only with groundwater evolution.
3) Monitoring the evolution of groundwater and soil movements at different monitoring points.
4) Comparing the groundwater and the soil movements measured with the predictions in order to validate the procedure. The efficiency of the BPW (to reduce soil movements) was also assessed by analysing the data obtained during the construction.

Note that other impacts not associated with the groundwater evolution (short term movements or large term movements caused after the tunnelling by creep or stress redistribution) should be estimated by geotechnical procedures. These topics were evaluated during the construction by a team of specialised scientists.

The aim of this paper is threefold: 1) to demonstrate the usefulness of new and advanced methods for hydrogeological impact quantification during tunnelling, 2) to propose a realistic methodology to improve the efficiency and reduce the risks during the construction of tunnels with an EPB in urban environments and 3) to describe the monitoring measures

taken during the HST tunnel construction (evolution of groundwater and soil movement) and discuss the main impacts arising from this construction.

2. General aspects

2.1. Characteristics of the construction

2.1.1. Proximity to Sagrada Familia

The Sagrada Familia is located in the centre of Barcelona (Figure 1). The area occupied by the landmark is approximately 12000 m^2 (one block of buildings) and its actual height is around 170 m (Figure 2). The HST tunnel, whose depth (in the study site) and radius are 30 and 5.8 m, respectively, passes at a distance of 10 m from the façade of the Sagrada Familia. The tunnel under the Sagrada Familia was dug in October 2010. There are two underground lines (Line 5 and Line 2), which are shallower than the HST tunnel, in the study area. Their depths are 12 m (Line 5) and 14 m (Line 2).

2.1.2. Bored Pile Wall (BPW)

A bored pile wall (BPW) was constructed to protect the Sagrada Familia from the movements caused by the EPB (Figure 2). The wall, which was formed by non secant piles, was 230 m long. The diameter of the piles was 1.5 m and they were 2 m apart. As a result, there was a gap of 0.5 m between each pair of piles. The depth of the wall was 41 m and the piles were built using reinforced concrete. The piles were constructed between August 2009 and April 2010. The characteristics of the BPW are described in detail by Rodríguez and Blanco (2012).

2.1.3. Padilla shaft

A maintenance shaft was excavated to repair and prepare the EPB at the crossroads between Mallorca and Padilla streets some 350 m from the Sagrada Familia (Figure 3). The shaft, whose diameter was 20 m, was excavated using the "cut and cover" method combined with deep pumping wells. The enclosure used for the excavation consisted of diaphragm walls from the surface to 46.5 m depth and of jet-grouting secant piles from 42.5 m to 61.5 m depth. The maximum excavation depth was 41 m and the drawdown inside the pumping wells needed to ensure stable (against bottom uplift) and dry conditions during the excavation stage was 45 m (58 m depth from the surface). Four pumping wells were used during the dewatering. The average of the total flow rate pumped was 12 l/s. The jet-grouting enclosure reduced the in situ permeability of the deep aquifer by a factor of 10 but still allowed a sizeable inflow (Pujades *et al.*, 2014a). As a result, the head fell outside the enclosure during dewatering. Aspects concerning the design and excavation of the shaft are explained in detail by Pujades *et al.*, 2014a.

2.2. Geology and geomorphology

2.2.1. General description

Barcelona is located in the NE of the Iberian Peninsula. The city is built on the Coastal Plain of the Catalan Coastal Ranges, which is a transition zone between the graben of Barcelona and the horsts of Garraf (West), Collserola (NW) and Montnegre (North) (Parcerisa et al., 2008). These horsts make up the Catalan Coastal Ranges. The city, which is also limited by the Mediterranean Sea (East), is between the rivers Besòs and Llobregat and extends to the lowest altitudes of the Coastal Range. The Geology of Barcelona is the result of

the superposition of the main geological events which have affected the Iberian plate and the Western Mediterranean since Ordovician times. Most of the outcrops in the urban area consist of Neogene sediments and Paleozoic rocks affected by the Variscan deformational, magmatic and thermal events. These sediments were unconformably overlain by Triassic rocks and subsequently deformed by the contractional structures of the Catalan Coastal Ranges which formed synchronously with the Pyrenees in the SE margin of the Ebro basin during Palaeogene times (Roca et al., 1999; Perea et al., 2006). Finally, the present landscape and geological configuration of the Barcelona urban area is the result of the late Oligocene-Neogene extensional event attributed to the opening of the Western Mediterranean. Extensional structures partially reactivated the Paleogene contractional and strike-slip faults (Roca and Guimerà, 1992; Sàbat et al., 1997; Santanach et al., 2011).

Some hills can be observed on the plain of Barcelona. Most of them are made up of Paleozoic materials (Horta, Guinardo, Gracia, Sant Gervasi and Sarria) and also of Miocene deposits (Montjuïc hill and Cathedral hill). The latter are constituted by Upper Miocene deltaic units (Gómez-Gras et al., 2001), which are separated from the Pliocene blue marls by the Messinian unconformity.

Two geomorphological units can be distinguished in the coastal plain: the Barcelona plain, where the study area is located, and the deltas of the rivers Besòs (Northeast) and Llobregat (Southwest). The two deltas are made up of quaternary materials and have similar characteristics. They are depositional systems, created during the Holocene, that consist of permeable formations (sands and gravels) separated by low hydraulic conductivity sediments (clays and silts; Velasco et al., 2012). Quaternary sedimentation in the two deltas has been mainly controlled by sea-level changes, Quaternary glaciations and fault activity (Gàmez et al. 2009). Quaternary materials in the the Besòs delta overlie over a substratum formed by Palaeozoic and Tertiary rocks. The Palaeozoic lithology consists mainly of slates and granite.

The Tertiary rocks are mostly made up of matrix-rich gravels and sandstones of Miocene age and of massive grey marls attributed to the Pliocene. The Quaternary of the Llobregat Delta River is deposited on top of Pliocene sediments.

Finally, the Barcelona Plain is mainly overlain by Pleistocene alluvial fans and Holocene near-shore and shore deposits (Riba and Colombo, 2009). The lower Quaternary deposits overlie the Pliocene series, which is formed by a regressive sequence composed of marine blue marls and sandy marls associated with gravel lenses that grade progressively into the lower Quaternary sediments. Fine sediments are predominant at the bottom of the Pliocene, whereas the number and thickness of layers with coarse sediments increase at shallower depths. Quaternary deposits can be divided into two: ancient Quaternary deposits, which are termed “tricycle” locally, and modern Quaternary. The “tricycle” is made up of three cycles which comprise, from bottom to top, red clays, yellow silts and calcareous muds and calcareous crust (Casassas and Riba, 1992). It increases in thickness from the higher altitudes (Collserola) towards the centre of the city. “The tricycle” is overlain by modern Quaternary, consisting of torrential, alluvial and foothill deposits, where gravels and sands with a high proportion of clay matrix are present.

At the Sagrada Familia (study site), the tunnel crosses mainly Pliocene materials, whereas the Padilla shaft crosses the Quaternary and the Pliocene (Figures 2 and 3).

2.2.1. Geological description of the study site

A detailed geological assessment was performed along the tunnel to determine the lithology, the lateral and vertical continuity of the sediments and the geometry of the geological structures (Figure 3 below). This was carried out by means of an accurate description of the materials from several fully cored boreholes that were drilled just before the

construction (Figure 3 above). These boreholes were interpreted together with descriptions and photos of former boreholes. Natural Gamma Ray logs were obtained to verify interpretations and depths. Figure 3 displays the detailed geological profile. The anthropogenic fill is 1-2 m thick in all the area except under the Sagrada Familia, where its thickness reaches 5 m. The Quaternary sediments, whose thickness varies along the profile from 20 to 1-2 m, are located below the fill. The Quaternary deposits consist of 1) clay with some gravel, 2) silt, and 3) sandy-silt. All Quaternary materials contain variable proportions of carbonate nodules. Continuous calcrete deposits were not observed at the study site as at other locations in Barcelona, where these deposits allow us to identify the series of the "tricycle". Discontinuous gravel deposits, which belong to paleochanels, were also observed in the Quaternary. The Pliocene materials are the deepest. They consist of alternating medium-fine sands, sandy marls and clayey marls. Fine materials are related to transgression events and coarse sediments to regression events. The Pliocene is affected by faults, one of which is located in the Cartagena street (Figure 3 below). The identification of this fault before the construction of the tunnel was of paramount importance given the different composition of the two sides. The EPB had therefore to be adapted to the new soil characteristics.

2.3. Hydrogeology

2.3.1. General description

Hydrogeologically, the Barcelona plain can be regarded as an aquifer with a high horizontal and vertical heterogeneity. Its effective transmissivity (T_{eff}) is 100-200 m^2/d. The hydraulic conductivity (k) of the Quaternary clay layers ranges from 0.001 to 0.01 m/d and the k of Quaternary sand and gravel layers varies from 0.1 to 10 m/d. The k of the Pliocene

fine materials ranges from 0.001 to 0.01 m/d. The *k* of the sand layers varies from 0.1 to 10 m/d. These values were derived from the numerous hydraulic tests performed during the HST tunnel project and other projects developed in Barcelona (Pujades *et al.*, 2014a, 2014b).

2.3.2. Pumping during the construction

Two pumping tests were performed near the Sagrada Familia (both at the Padilla shaft). The first test (August 2009) lasted 4 days (two for pumping and two for recovery). Water was pumped from one well screened from the water table (located at 13 m depth) to 40 m depth. The maximum drawdown reached in the well was 6 m, and the average flow rate was 5 l/s. Two pumping wells were used in the second test (January 2010), when the enclosure was partially constructed. The test lasted 5 days (2 for pumping and 3 for recovery). The maximum drawdown reached in the well was 11 m and the average flow rate was 10 l/s. The hydraulic parameters of the aquifer were obtained from these tests (Pujades et al., 2014a), that were interpreted using the finite element code TRANSIN-IV (Medina and Carrera, 1996, 2003; Medina *et al.,* 2000) with visual interface of VISUAL TRANSIN (UPC, 2003). The code performs automatic estimation (also termed inverse problem or back analysis) using the Levenberg-Marquardt algorithm (Carrera and Neuman 1986a, 1986b, 1986c).

Three more pumpings were performed at the Padilla shaft, one to characterise the jet-grouting enclosure hydraulically (May 2012, 2 days for pumping and 2 for recovery), a second to dewater the excavation (June 2010, 25 days) and a third to facilitate the entry of the EPB into the Padilla shaft (August 2010, 10 days). In the first pumping, the drawdown at the pumping well, which was located inside the excavation, achieved 18 m and the average flow-rate was 5 l/s. During the dewatering performed in June 2010, the maximum drawdown inside the excavation was 50 m. Finally, the drawdown was also 50 m during the third pumping

which was performed using six pumping wells located outside the enclosure. The considerable drawdown produced was essential to allow the entry of the EPB into the enclosure without problems.

2.3.3. Groundwater at the study site

Different piezometers were installed at the Sagrada Familia to determine the behaviour of groundwater at the study site (Figure 4). The piezometers were screened at different depths. Most of them were screened completely but some were screened only in the deepest layers. Table 1 shows the depth where the piezometers were screened and the position of the hydraulic head (m.a.s.l.) prior to the construction. Note that the position of the hydraulic head could vary owing to errors in the assignment of the level to the top casing of each piezometer. However, the errors are not large. Measurements show that the hydraulic head varied with depth. The hydraulic head was located at 13-14 m.a.s.l. (17.5-16.5 m in depth) at piezometers screened in the layers shallower than 30 m depth (they are shaded in the table) whereas hydraulic head pressure was greater in the deeper layers. The hydraulic head reached 15-17 m.a.s.l. (15.5-13.5 m in depth) at the piezometers screened in the layers deeper than 30 m. Figure 3 shows two layers (dashed black line) of fine materials (marls and clays with some fine sands), located more or less at 30 m depth, which would separate hydraulically the upper layers from the lower ones. It would be possible to regard the upper layers and the lower ones as independent aquifers (only in the study site). The upper aquifer (upper layers) would be unconfined while the lower one (lower layers) would be confined. Note that the difference of hydraulic head between the upper and the lower layers would be greater under natural conditions. However, before taking these measures, some piezometers had been drilled, connecting all the layers and reducing the differences of the hydraulic heads. This variation of

the hydraulic head with depth was also observed during the construction of the Padilla shaft. This information was crucial because the EPB was subjected to a much higher water pressure from the layers under the tunnel.

2.4. Soil overconsolidation

The overconsolidation ratio (OCR) of the soil is essential to predict soil movements caused by groundwater oscillations. The hydraulic heads fell in Barcelona during the 1960s because of heavy pumping (Vázquez-Suñè, *et al.,* 2005). They recovered as pumping within the city was abandoned. But the net effect was a significant increase in the OCR in all the sediments. As a result, pumping settlements should be small and the soil should behave elastically in response to groundwater oscillations when these are smaller than the maximum drawdown caused in the past (Pujades, *et al.*, 2014a, 2014b). Groundwater fluctuations larger than the maximum historical drawdown would cause unrecoverable movements. Historical hydraulic head data and a numerical hydraulic head evolution were used to determine the magnitude of the groundwater oscillations in the past (Figure 5). Numerical hydraulic head evolution was obtained from the numerical model of Barcelona (Vázquez–Suñé *et al.*, 1997, 1999a, 1999b, 2005). This model, which is supported by hydraulic head measurements available in the proximity of the Sagrada Familia since 1950, includes data from historical recharge, pumpings and underground constructions. The hydraulic head evolution near the Sagrada Familia was obtained and compared with the historical data. Some differences can be observed between the historical and the numerical hydraulic heads. These occur because the model of Barcelona is regional and considers the entire city. Therefore, some local variables such as the location of punctual leakages towards underground structures or the flowrate of some pumping wells are not properly known. However, the objective of the Figure 5 is to

show the groundwater oscillations in the past to justify that the soil in the study site is overconsolidated. Note that the piezometers where the historical data were taken are not the same than the use during the construction.

The head underwent significant variations in the last century. It was 15 m lower in the 1960s and reached a maximum at the start of the 1990s.The hydraulic head is currently located 4 or 5 m below this maximum. The characteristics of the HST tunnel construction suggested that groundwater oscillations during (and after) the works would be smaller than the historical oscillations. Soil movements due to groundwater variations would therefore be small and elastic and should not pose a risk to the Sagrada Familia or to the buildings adjacent to the study site.

3. Analysis and impact assessment

3.1. Hydrogeological predictions

The barrier effect (s_B) is the increase in head loss along the flow lines caused by the reduction in conductance attributed to the construction of an impervious underground structure (Pujades et al., 2012b). Therefore,

$$s_B = \Delta h_B - \Delta h_N \qquad (1)$$

where Δh_B is the head drop across the barrier and Δh_N is the head drop between the same points under natural conditions.

Given that the magnitude of s_B depends on the location, two types of barrier effect can be distinguished: the local barrier effect (s_{BL}) and the regional barrier effect (s_{BR}). The local barrier effect is the maximum head rise (or drop) which occurs close to the barrier, while the regional effect is the impact observed at some distance from the barrier (Pujades et al.,

2012b). The arrangement of the impact depends on the boundary conditions of the aquifer. If the hydraulic head is prescribed downgradient, the barrier effect is accumulated upgradient and viceversa. When the conditions of the boundaries of an aquifer are not of prescribed head, the hydraulic head behaves ideally, rising upgradient and dropping symmetrically downgradient (Pujades et al., 2012b).

The barrier effect (local and regional) can be computed analytically or numerically. Pujades et al., (2012b) proposes analytical equations to compute the s_B caused by different types of barrier. These equations allow us to compute the total head loss caused by the barrier (underground construction) but not its arrangement across the aquifer.

Two barrier effects were expected and predicted analytically at the study site: 1) the impact caused by the BPW and 2) the effect produced by the tunnel. From the equations proposed by Pujades et al., (2012 b), those for partial barriers (Equations 2, 3 and 4) were used since both structures (BPW and tunnel) can be regarded as partial barriers. The BPW was considered to be a partial horizontal barrier (Figure 6a) whereas the tunnel was assumed to be a partial vertical barrier (Figure 6b). Each pile of the BPW can be regarded as a different partial horizontal barrier since two no flow boundaries, perpendicular to the barrier, can be differentiated: one in the middle of each pile and the other in the middle of the gap between each pair of piles (Figure 6). Note that the maximum local barrier effect will be observed in the middle of each pile and this will be the same in all the piles. Equations 2 and 3 allow us to compute the regional (s_{BRO}) and the local (s_{BLO}) barrier effects produced between the boundary of the aquifer and the barrier whereas Equation 4 enables us to compute the head loss produced when the groundwater flows under or round the barrier (s_{BI}) (depending on the length partially cut by the barrier). The total impact is obtained by adding both values (s_{BRO} or $s_{BLO} + s_{BI}$).

$$s_{BRO} = \begin{cases} 0 & if \quad b_{bD} \le 0.1 \\ \dfrac{2 i_N b}{3\pi} \ln\left(\dfrac{1}{5\pi b_{bD} \left(1 - b_{bD}\right)^6} \right) & if \quad b_{bD} > 0.1 \end{cases} \qquad (2)$$

$$s_{BLO} = \begin{cases} 2 b_{bD} i_N b & if \quad b_{bD} < 0.28 \\ i_N b \sqrt{\dfrac{3}{8}} \ln\left(\dfrac{2 {b_{bD}}^{0.29}}{{b_{aD}}^2} \right) & if \quad b_{bD} \ge 0.28 \end{cases} \qquad (3)$$

$$s_{BI} = i_N L_B \left(\frac{b}{b_a} - 1 \right) \qquad (4),$$

where L_B is the width of the barrier, i_N is the natural groundwater gradient perpendicular to the barrier measured before the construction of the barrier, b is the thickness of the aquifer (or width, depending on the length partially cut by the barrier), b_a and b_b are the open and cut fractions of the aquifer, respectively, and finally, $b_{bD} = \left(b_b / b\right)$ and $b_{aD} = \left(b_a / b\right)$ are open and cut fractions of the aquifer expressed in dimensionless form. Note that the distances (b_a and b_b) must be corrected when the soil is heterogeneous in the direction followed by the flow to cross the barrier. Therefore, given the vertical heterogeneity of the soil, these distances were corrected using the anisotropy factor to compute the barrier effect caused by the tunnel. The anisotropy factor (12) was obtained from the hydraulic characterisation of the site. The natural groundwater gradient used for the analytical predictions was 0.01, which was obtained from the hydrogeological numerical model of Barcelona (Vázquez–Suñé *et al.*, 1997, 1999a, 1999b, 2005). Piezometric contour lines (in natural conditions) obtained from this model are displayed in Figure 4. Observations of available piezometers were not used since these could be perturbed by aspects related with the construction.

The barrier effects caused by the BPW and by the tunnel were computed using the distances shown in Figure 6 and in Equations 2, 3 and 4, The regional and local barrier effects

predicted for the BPW were 0.057 and 0.06 m, respectively, whereas the regional and the local barrier effects expected for the tunnel were 0.2 and 1.5 m, respectively.

The barrier effect caused by the tunnel had also been predicted numerically years ago of the construction (GHS-UPC, 2000). A multilayered numerical model, which represents the aquifers in Barcelona, had been used. The validity of this model had been tested since it had been used to solve other hydrogeological problems in Barcelona. The tunnel had been implemented as an impervious structure which crossed Barcelona and cut half of the aquifer to compute the hydrogeological impacts. The results, which were obtained in steady state, showed that the maximum barrier effect would be 1.25 m, and would be concentrated in areas located close to the tunnel (maximum local barrier effect). By contrast, far from the tunnel, the barrier effect would be close to 0.5 m (regional barrier effect). The model also showed that the majority of the barrier effect would accumulate downgradient. The drop caused by the local barrier effect downgradient would be 1 m while the rise upgradient would be less (0.25 m). A general view of the numerical results is displayed in the on-line appendix. The contour lines show the differences between the hydraulic head in natural conditions and the hydraulic head after the construction of the tunnel.

The analytical and numerical predictions of the barrier effect caused by the tunnel were similar. Note that the numerical and the analytical predictions for the barrier effect also agreed with the measures taken by Culí (2011) at other sites of the tunnel (s_B = 1.8 m of which 1.3 m occurred downgradient). All the results are given in Table 2.

3.2. Soil displacement predictions

Groundwater oscillations may cause soil settlements or heaves. Settlements due to groundwater fluctuations were calculated from model drawdowns as (Cashman and Preene, 2001)

$$\rho = \gamma_W s D \alpha \quad (4)$$

where ρ is the settlement, γ_W is the specific weight of water (10 kN/m^3), s is the head drop (m), D is the thickness (m) of the aquifer and α is the soil compressibility (kP$_a^{-1}$). All terms are known except α, which can be derived from the storage coefficient of the aquifer (S) because the soil in Barcelona is overconsolidated and behaves elastically (Pujades, *et. al.*, 2014a, 2014b). Thus, α can be determined from

$$S_i = \gamma_W \theta_i D_i \left(\beta + \frac{\alpha_i}{\theta_i} \right) \quad (5)$$

where θ is the porosity and β is the water compressibility. It is possible to consider that $S_S = \alpha$, assuming that β is very small compared to α, where S_S is the specific storage coefficient, which can be obtained from the interpretation of pumping tests. Settlements were computed by assuming a value of S_S of 10^{-5} m^{-1}, derived from the pumping tests performed during the construction. Although this methodology assumes exclusively vertical movements, which is not always the case, it allows us to approximate the displacements with an acceptable error (Pujades et al., 2014a).

Soil movements induced by the barrier effect caused by the construction were computed. The nature of the soil movements depends on the side of the barrier where they are observed. Ideally, the barrier effect produces a heave of the groundwater upgradient and a symmetrical drop downgradient with the result that the soil will heave upgradient and settlements will occur downgradient. However, it should be noted that the distribution of the barrier effect is determined by the boundary conditions (as at the study site). Therefore, the

barrier effect is assessed by determining the increase in the head drop through the barrier (adding the increase upgradient and the drop downgradient). Consequently, the soil movements caused by the barrier effect were evaluated in the same way, i.e. the value computed, which can be termed “total soil movement”, reflects the heave produced upgradient and the settlement downgradient. The total soil movement can be obtained by adding the heave upgradient and the settlement downgradient and was computed by replacing the drawdown (s) by the predicted barrier effect in Equation 4. Note that in this paper, the term “total soil movement” only considers those displacements caused by variations of the groundwater. Soil movements caused by other causes are not regarded.

The total soil movement caused by the barrier effect of the tunnel was computed using the numerical and the analytical predictions. The maximum displacement using the numerical results (local barrier effect) was 0.54 mm, while regionally, the calculated movement was 0.22 mm. Displacements obtained using the analytical groundwater predictions were 0.65 mm (local barrier effect) and 0.08 mm (regional barrier effect). Finally, the total soil movement caused by the BPW was also calculated using the analytical predictions. The maximum total movements predicted locally and regionally were 0.026 and 0.025 mm, respectively. Displacements were not large since the predicted groundwater fluctuations were small. The results are given in Table 2.

4. Monitoring and impact quantification

4.1. Groundwater monitoring

The heads were measured manually and automatically at several piezometers located around the Sagrada Familia (Figure 4). The characteristics of these piezometers are shown in Table 1. The great majority were screened completely with the exception of the piezometers

PZ-5, PZ-11 and PZ-12, which were screened only in deep layers. Figures 7 and 8 display the hydraulic head variations during the construction upgradient and downgradient, respectively.

4.1.2. Impact of the BPW construction

During the construction of the BPW, the hydraulic head rose at three piezometers (0.35 m at PZ-16, 0.28 m at PZ-14 and 0.17 m at PZ-13) located upgradient and fell at two (0.32 m at PZ-6 and 0.75 m at PZ-5) located downgradient. This behaviour accorded with a barrier effect caused by the BPW. However, the hydraulic head observed at other piezometers suggested that the cause of the groundwater oscillation could be different since drops (0.33 m at PZ-4, 0.5 m at PZ-11 and 0.15 m at PZ-4) were observed upgradient and one increase (0.31 m at PZ-18) was measured downgradient. The hydraulic connection between layers with different hydraulic heads was responsible probably for the groundwater behaviour around the Sagrada Familia during the construction of the BPW. As stated above, the hydraulic head in the deeper layers was higher than in the shallower ones. Therefore, the construction of the piles would have connected all the layers hydraulically, causing a drawdown in the deeper layers and an increase in the shallower ones. In fact, the hydraulic head fell at all the piezometers whose screens reached layers deeper than 30 m and the head rose at the piezometers screened in shallower layers. The behaviour of the hydraulic head at each piezometer (due to the construction of the BPW) is depicted by a symbol in Table 1.

The connection between layers with different hydraulic heads caused by the construction of the piles can be best observed at the piezometers PZ-11 (upgradient) and PZ-5 (downgradient; Figure 9). Initially, we believed that the cause of the drop was the second pumping test of Padilla since the two events were simultaneous. However, the drawdown lasted longer than the test (January 2010 until April 2010). These piezometers were located

near the BPW (Figure 9a) and four abrupt drops (Figure 9b) were observed at PZ11, which coincided with the construction of four piles (P59, P57, P55 and P56) close to the piezometers. The relationship between the piles and the drops was more visible at PZ11. The sudden drop in hydraulic head could also be attributed to a decompression of the soil caused by the excavation of the piles. However, this should not have lasted long. The most likely cause is the hydraulic communication between layers with different hydraulic heads.

Thus, if a barrier effect was created by the BPW, it could not be differentiated from the oscillations produced by other causes associated with the construction of the BPW. In fact, the barrier effect predicted was considerably smaller than the variations of head produced by the hydraulic connection between the layers. Note that the behaviour observed could not have been caused by natural groundwater oscillations (±0.7 m according to the historical record) since the groundwater behaved differently at each piezometer.

4.1.3. Barrier effect caused by the tunnel

EPB drilling causes head oscillations, the magnitude of which depends on the hydraulic properties of the soil. If the oscillations are high, the water may spring up to the surface from the piezometers nearby. Therefore, the piezometers near the tunnel were sealed before the passage of the EPB so as to allay the fears aroused by the construction (when the drilling of the tunnel commenced, a water jet welled up from one piezometer causing alarm among the neighbours). Only some piezometers, which were located at some distance from the tunnel, were preserved. As a result, during the tunnel construction around the Sagrada Familia, it was only possible to take measurements at three piezometers (PZ-3, PZ-15 and PZ-19). A drop of 1.6 m was measured when the tunnel was constructed at the piezometer located downgradient (PZ-19) whereas the heads in the upgradient piezometers (PZ-3 and PZ-15)

returned to their initial position. This distribution (most of the impact concentrated downgradient) was predicted by the numerical analysis. The magnitude of the barrier effect also correlated well with the numerical and analytical predictions. The measurements were similar to the barrier effect observed at other sites of the construction (Culí, 2011). Note that the hydraulic head rose at PZ-6 (located downgradient) when the EPB passed, but its evolution was not measured after the construction because the piezometer was sealed. Although the hydraulic head evolution observed at PZ-6 and PZ-19 (both located downgradient) was different during the pass of the EPB, their evolution was probably similar once the tunnel was constructed. As a result, the hydraulic head after the pass of the EPB would have also dropped at PZ-6.

4.1.4. Drain effect

After the construction of the tunnel there was no drain effect. No inflows were observed in the tunnel and the head did not drop near the tunnel after construction, suggesting that there were no serious defects in the lining of the tunnel.

4.1.5. Pumping at the Padilla shaft

Hydraulic head evolutions at the piezometers of the Sagrada Familia (Figures 7 and 8) show that only the effects of three of the five pumpings performed at the Padilla shaft were detected. These were the two first pumping tests, performed prior to the completion of the enclosure, and the last dewatering, performed to facilitate the entry of the EPB into the shaft. The other pumpings were not detected since they were performed inside the enclosure, which

had been deepened more than was structurally necessary (using jet-grouting piles) because of the fears caused by the pumping settlements (Pujades et al., 2014a).

The first pumping test at the Padilla shaft caused a maximum drawdown of 0.2 m, which was measured at PZ-12, PZ-11 and PZ-19. The drawdown at the other piezometers was lower. The maximum drawdown observed during the second pumping test was higher (0.3 m) and was detected at piezometers PZ-6, PZ-13 and PZ-11. During the last pumping, few piezometers were available since most of them were sealed. The maximum drop, which was 0.6 m, was observed at piezometer PZ-13. In summary, the effects of pumping in the Padilla shaft were observed at the Sagrada Familia site. However, the drawdown caused was too low to give rise to significant movements of the soil.

4.2. Monitoring of settlements

Only the settlements measured during the passage of the EPB under the Sagrada Familia are analysed here. The construction of the BPW and other works undertaken may have generated soil movements, but data are not available. Three parallel rows of monitoring points were located in front of the Sagrada Familia (Figure 10). One row was located upgradient, another just above the tunnel and the last row downgradient. Note that the BPW was located between the tunnel and the upgradient monitoring points. Soil displacements were studied by comparing the movement at the three rows (upgradient, above the tunnel and downgradient) in five sections (A, B, C, D and E in Figure 10). Soil movements at three of these sections are displayed in Figure 11 (Sections B, D and E). Each pair of plots belongs to one of these sections. The upper plots display the evolution of the soil movement from just before the arrival of the EPB at the Sagrada Familia (9-10-2010) until the end of the monitoring (1-3-2011), and the lower ones show a zoom of the soil movements only during

the passage of the EPB under the Sagrada Familia (from 9-10-2010 to 18-10-2010). Note that the soil movements in Sections A and C are not included in Figure 11. This is because the soil movements coincided with those of Section B. However, the results obtained in all the sections (Sections A to E) are given in Table 3. There is a clear distinction between short and long term movements. Short term movements (lower plots) are related to construction operations such as ground loss during excavation, grout injection or the pushes performed by the EPB to advance. The displacements consist of a sharp drop (point 1 in the plots) followed by a rise and a subsequent prolonged drop (point 2 in the plots). This evolution was observed at all the monitoring points. The drops would correspond to ground loss and the heaves to grout injections. The maximum settlements caused during the tunnel excavation (points 1 and 2 in the plots) are given in Table 3. The total soil movements were small and similar on both sides of the tunnel, which suggests that the BPW was not efficient in preventing settlements. However, its efficiency is difficult to evaluate since movements were too small to be measured accurately. The reduction of movement upgradient due to the BPW can be best observed in the plots shown by Rodríguez and Blanco (2012). They show the maximum displacements measured in sections perpendicular to the tunnel.

Small and sharp oscillations which occurred during the short term movements were associated with the advance of the EPB. Soil rises whenever the EPB pushes the soil to advance and drops when the EPB comes to a halt. Each push of the EPB modifies the structure of the soil near the machine, reducing its porosity. This causes an increase in the hydraulic head, which returns to its initial position when the push ceases. Therefore, the relationship between the pushes to advance and the movements of the soil can be demonstrated by comparing the head and the soil movements during the tunnel drilling. The data from one piezometer and from three soil monitoring points located near the Sagrada Familia were used for this purpose (Figure 12a and Figure 12b). High frequency head

oscillations, which were caused by the advance of the EPB, matched the soil movements. This type of soil movement was observed on both sides of the BPW since the wall was not designed to reduce it. The effects of reducing the storage capacity of the soil by compressing it are easily transmitted to the surroundings of the EPB.

The second type of soil displacement was a long term movement, which may take between a few months and a few years to reach a steady state (Ercelebi *et al.*, 2011). This movement was evaluated using the data between December and March 2011 (last measurement). This period is depicted by number 3 and an arrow in the upper plots of Figure 11. Long term movements are generally associated with creep, stress redistribution and consolidation of the soil after drainage of groundwater (dissipation of water pressure; Ercelebi *et al.*, 2011). However, soil consolidation due to the redistribution of the water pressure as a result of the interaction between the aquifer and the tunnel (barrier effect) should also be considered. The movements observed were probably due to a combination of factors. The plots show that the long term effects acted differently upgradient and downgradient. Soil heaved upgradient and settled (or heaved less) downgradient, which suggests that most of the movements were caused by the barrier effect. Displacements were compared with the predictions (section 3.2 of this paper) by adding the maximum heave upgradient and the maximum settlement downgradient (to obtain the total soil movement) in the different sections of the monitoring points (Figure 11). The predictions (0.54 – 0.65 mm) were similar to the observations (from 0.11 mm in section A to 0.72 mm in section C). The differences between them could be due to long term movements associated with the other factors that would not have affected upgradient and downgradient in the same way. The BPW could have prevented some factors from affecting upgradient. If other factors unrelated to the barrier effect had affected both sides of the tunnel equally, the displacements predicted for the barrier effect would have matched the measured ones.

It should be pointed out that the movements measured just above the tunnel were not used in Table 3 to evaluate the soil displacements caused by the barrier effect since this location was severely affected by the excavation of the tunnel.

The evolution of spatial distribution of soil movements caused by the tunnel construction was also studied in different stages (Figure 13). This figure represents the total movements measured by the monitoring points since their installation. Figure 13a shows the soil position when the EPB was in Marina street (just before the start of the drilling under the Sagrada Familia) and Figure 13b indicates the movement when the EPB had passed Sardenya street (just after the drilling under the Sagrada Familia). Figures 13c to 13f display the distribution of soil movement one (Figure 13c), two (Figure 13d), three (Figure 13e) and four (Figure 13f) months after the excavation of the tunnel under the Sagrada Familia. As the EPB approached the Sagrada Familia, it caused a heave (depicted by triangles in the Figures). This heave was produced by the pressure applied over the soil during the drilling. However, as the EPB moved away, the ground settled (settlements are depicted by circles in the figures). The soil continued to settle for two months after the passage of the EPB. This settlement could be due to the reduction in horizontal stresses in the tail of the EPB. However, soil recovered somewhat during the third and the fourth months after drilling (mainly upgradient). This last recovery was associated with long term movements. This is also observed in Figure 14, where the variations from December to January (Figure 14a) and from December to March (Figure 14b) are shown. The barrier effect was partly responsible for this behaviour because the soil heaved upgradient while it settled or heaved to a lesser degree downgradient.

5. Discussion and conclusions

The construction of the HST tunnel across Barcelona aroused a great deal of controversy. The fact that the tunnel passed close to the Sagrada Familia Basilica attracted the attention of politicians and the media. Such was the alarm that a committee appointed by the UNESCO acted as external observers. As a result, the safety measures were increased during the construction to forestall any unexpected events. The present study demonstrates the usefulness of hydrogeological impact quantification methods for tunnelling and proposes a realistic methodology to improve efficiency and mitigate risk during the construction of tunnels with EPB in urban environments. The study also discusses the monitoring measures taken during the HST tunnel construction and considers the main impacts of this construction. Impacts not related with the groundwater (most of the movements caused by tunnelling) were also predicted by specialised scientists in this field. Their studies were equally necessary to ensure the suitability of the construction.

It goes without saying that predictions about impacts due to an underground construction must be made given that, if the impacts are large, the construction must be redesigned. It is essential to characterise the soil in order to make satisfactory predictions. The soil of the study site was therefore characterised hydrogeologically using different techniques (borehole logging, Natural Gamma Ray and pumping tests).

The main hydrogeological impact expected was a barrier effect. A numerical and new analytical tools were used to predict the barrier effect, and the predictions matched the measures taken during the construction. Both the magnitude and the distribution of the barrier effect were estimated. In general, hydrogeological impacts caused by the tunnel were acceptable and corrective measures to reduce the barrier effect were not necessary. The maximum head drop due to the barrier effect produced by the tunnel was 1.6 m. Note that this impact was local and probably decreased further away from the tunnel.

An unpredicted groundwater behaviour produced by the construction of the EPB was observed. This was caused by the connection of layers with different hydraulic heads. Drawdowns were observed in deep layers and increases in the shallower ones. This effect was greater than the maximum barrier effect (produced by the BPW) expected. It was not possible therefore to detect the barrier effect caused by the BPW and to validate the analytical predictions made for the wall.

Two types of soil movements, short and long term, were observed during the drilling of the tunnel. The short term movements were related to the ground loss and the grout injection during the excavation of the tunnel and to the pushes of the EPB over the soil to advance. These pushes produced sharp oscillations of the soil which matched the high frequency head variations observed during the passage of the EPB. The long term movements, which were estimated analytically, were mainly due to the redistribution of water pressure produced by the interaction between the tunnel and the groundwater (barrier effect). Other factors such as stress redistribution after drilling contributed to the long term movements but to a lesser degree. This fact does not always occur and in other constructions long term movements not related with the groundwater evolution can be greater or even dangerous. For this reason, these must always be estimated by geotechnical methods as was undertaken before the construction of the HST tunnel in Barcelona.

The safety measures adopted (during the HST tunnel construction) such as the BPW or intensive monitoring added considerably to the cost of the construction. However, given the location of the tunnel (adjacent to the Sagrada Familia) these measures considerably mitigated the risks. The BPW helped to allay fears. Monitoring allows us to follow the evolution of the works and to improve our knowledge of constructing tunnels using EPBs.

The methods employed during the HST tunnel construction in Barcelona proved to be appropriate and useful in assessing impact since the predictions agreed with the observations.

Numerical and analytical tools are suitable for computing the hydrogeological impacts with a moderate degree of error. But these tools depend on a detailed characterisation to obtain the best results. Soil displacements caused by groundwater oscillations can be readily calculated by using simple analytical equations. Naturally, if a coupled hydro-mechanical model is used, the estimations will be better. However, occasionally data and time needed to construct a reliable model are not available, and in such cases analytical equations will be helpful.

6. Acknowledgements

The authors would like to acknowledge ADIF (Administration), SACYR (Construction company) and INTECSA-INARSA (Technical assistance) for their support throughout the hydrogeological monitoring of the civil works. The authors were appointed by ADIF as external advisors during the construction of the tunnel. Additional funding was provided by Spanish Ministry of Science and Innovation (MEPONE project: BIA2010-20244); and the Generalitat de Catalunya (Grup Consolidat de Recerca: Grup d'Hidrologia Subterrània, 2009-SGR-1057). E. Pujades gratefully acknowledges the financial support from the AGAUR (Generalitat de Catalunya) through “the grant for universities and research centres for the recruitment of new research personnel (FI-DGR)”.

7. References

Butscher, C., 2012. Steady-state groundwater inflow into a circular túnel. Tunelling and underground space technology. 32, 158-167.

Carrera, J., Neuman, S., 1986a. Estimation of aquifer parameters under transient and steady state conditions: 1. Maximum likelihood method incorporating prior information. Water Resources Research, 22 (2), 199-210.

Carrera, J., Neuman, S., 1986b. Estimation of aquifer parameters under transient and steady state conditions: 2. Uniqueness, stability and solution algorithms. Water Resources Research, 22 (2), 211-227.

Carrera, J., Neuman, S., 1986c. Estimation of aquifer parameters under transient and steady state conditions: 3. Application to synthetic and field data. Water Resources Research, 22 (2), 228-242.

Casassas, L., Riba, O., 1992. Morfologia de la rambla Barcelonina. Treballs de la Societat Catalana de Geografia, 33-34 (7), 9-23.

Cashman, P.M., Preene, M., 2001. Groundwater lowering in construction – A practical guide. Spon press, London.

Chae, G.T., Yun, S.T., Choi, B.Y., Yu, S.Y., Jo, B.M., Kim, Y.J., Lee, J.Y., 2008. Hydrochemistry of urban groundwater, Seoul, Korea: The impacto f Subway tunnels on groundwater quality. Journal of Contaminant Hydrology. 101, 42-52.

Cia, B., Blanchar, C.,. El País digital [on-line]. 28 January 2005. [Consult date: 10 January 2014]. Available in: <http://elpais.com/diario/2005/01/28/espana/1106866824_850215.html>.

Culí, L, 2011. Estudio de la relación entre el funcionamiento de una tuneladora (EPB) con la geología del terreno y las variaciones del nivel piezométrico. Minor thesis. Universitat Politècnica de Catalunya.

Custodio, E., Carrera, J., 1989. Aspectos generales sobre la contaminación de las aguas subterráneas. OP. 13, 96-112.

Deveughèle, M., Zokimila, P., 2010. Impact of an impervious shallow gallery on groundwater flow. Bulletin of Engineering Geology and the Environment. 69, 143-152.

El Tani, M., 1999. Water inflow into tunnels. In: Alten, et al. (Ed.), Challenges for the 21st Century. Balkema, Rotterdam, pp. 61–70.

El Tani, M., 2003. Circular tunnel in a semi-infinite aquifer. Tunnelling and Underground Space Technology 18, 49–55.

Ercelebi, S.G., Copur, H., Ocak, I., 2011. Surface settlement predictions for Istanbul Metro tunnels excavated by EPB-TBM. Environmental Earth Science. 62, 357-365.

Gàmez, D., Simó, J.A., Lobo, F.J., Barnolas, A., Carrera, J., Vázquez-Suñé, E., 2009. Onshore-Offsore correlation of the Llobregat deltaic system, Spain: Development of deltaic geometries under different relative sea-level and growth fault influences. Sedimentary Geology 217, 65-84.

GHS-UPC, 2000. Evaluación del impacto hidrogeológico del Tren de Alta Velocidad a su paso por el Delta del Llobregat y por la ciudad de Barcelona. Technical report for INTRAESA-GIF. Barcelona, Spain.

Gómez-Gras, D., Parcerisa, D., Calvet, F., Porta, J., Solé de Porta, N., Civis, J., 2001. Stratigraphy and petrology of the Miocene Montjuïc delta (Barcelona, Spain). Acta Geologica Hispanica, 36 (1-2), 115-136.

Goodman, R.F., Moye, D.G., Van Schaikwyk, A., Javandel, I., 1965. Groundwater inflows during tunnel driving. Bulletin of the Association of Engineering Geologists. 2 (1), 39–56.

Jimenez, R., Senent, S., 2012. Teaching the importance of engineering geology using case histories, in: McCabe, Pantazidou and Phillips (Eds.), Shaking the foundations of Geo-Engineering education. Francis and Taylor Group, London, pp. 99-104.

Kolymbas, D., Wagner, P., 2007. Groundwater ingress to tunnels – The exact analytical solution. Tunelling and underground space technology. 22, 23-27.

Kusumoto, S., Omae, H., Sato, T., Watanabe, M., Kobayashi, N., Nishida, K., 2003. Construction of preservation facilities on natural groundwater flows, in: Kono, Nishigaki and Komatsu (Eds.), Groundwater Engineering – Recent Advances. Swets and Zeitlinger, Lisse, pp. 237-242.

Li, H., Kagami, H., 1997. Groundwater level and chemistry changes from túnel construction near Matsumoto City, Japan. Environmental Geology. 31, 76-84.

Marinos, P., Kavvadas, M., 1997. Rise of the groundwater table when flow is obstructed by shallow tunnels, in: Chilton, J. (Eds.), Groundwater in the urban environment: Problems, processes and management. Balkema, Rotterdam, pp. 49-54.

Medina A, Carrera J, 1996. Coupled estimation of flow and solute transports parameters. Water Resources Research, 32 (10), 3063-3076.

Medina, A., Alcolea, A., Carrera, J., Castro, L.F., 2000. Modelos de flujo y transporte en la geosfera: Código TRANSIN IV. [Flow and transport modelling in the geosphere: The code TRANSIN IV]. IV Jornadas de Investigación y Desarrollo Tecnológico de Gestión de Residuos Redioactivos de ENRESA. Technical publication 9/2000: 195-200.

Medina A, Carrera J, 2003. Computational different type of data Geostatistical inversion of coupled problems: dealing with computational burden and different types of data. Journal of Hydrology, 281 (4), 251-264.

Meiri, D., 1985. Unconfined groundwater flow calculation into a tunnel. Journal of Hydrology 82, 69–75.

Melis, M., 2005. The collapse of a railway tunnel by face instability in soft or very fractured rocks and soils (Second part). Revista de Obras Públicas, 3458, 7-24.

Ni, J., C., Cheng, W., 2011. Shield machine disassembly in grouted soils outside the ventilation shaft: A case history in Taipei Rapid Transit System (TRTS). Tunnelling and Underground Space Technology, 26, 435–443.

Parcerisa, D., Gámez, D., Gómez-Gras, D., Usera, J., Simó. J.A., Carrera, J., 2008. Estratigrafía y petrología del subsuelo precuaternario del sector SW de la depresión de Barcelona (Cadenas Costaro Catalanas, NE de Iberia). Revista de la Sociedad Gaológica de España, 21 (3-4), 93-109.

Paris, A., Teatini, P., Venturini, S., Gambolati, G., Bernstein, A.G., 2010. Hydrological effects of bounding the Venice (Italy) industrial harbour by a protection cut-off wall: a modeling study. Journal of Hydrologic Engineering. 15 (11), 882–891.

Perea, H., Masana, E., Santanach, P., 2006. A pragmatic approach to seismic Parameters in a region with low seismicity: The case of Eastern Iberia. Natural Hazards, 39, 451-477.

Pujades, E., Carrera, J., Vázquez-Suñé, E., Jurado, A., Vilarrasa, V., Mascuñano-Salvador, E., 2012a. Hydraulic characterization of diaphragm walls for cut and cover tunnelling. Engineering Geology. 125, 1-10.

Pujades, E, López, A., Carrera, J., Vázquez-Suñé, E., Jurado, A., 2012b. Barrier effect of underground structures on aquifers. Engineering Geology, 145-146, 41-49.

Pujades, E., Vázquez-Suñé, E., Carrera, J., Vilarrasa, V., Jurado, A., De Simone, S., Ledesma, A., Ramos, G. Lloret, A., 2014a. Deep enclosures versus pumping to reduce settlements during shaft excavations. Enginnering Geology, 169, 100-111.

Pujades, E., Vázquez-Suñé, E., Carrera, J., Jurado, A., 2014b. Dewatering of a deep excavation undertaken in a layered soil. Enginnering Geology. Doi: 10.1016/j.enggeo.2014.06.007

Riba, O., Colombo, F., 2009. Barcelona: la Ciutat Vella i el Poblenou. Assaig de geologia urbana. Institut d'Estudis Catalans – Reial Acadèmia de Ciències i Arts de Barcelona, Barcelona, 278 pp.

Ricci, G., Enrione, R., Eusebio, A., 2007. Numerical modelling of the interference between underground structures and aquifers in urban environment. The Turin subway – Line 1, in: Barták, Hrdine, Romancov and Zlámal (Eds.), Underground Space. Taylor and Francis Group, London, pp. 1323-1329.

Roca, E., Sans, M., Cabrera, L., Marzo, M.,1999. Oligocene to Middle Miocene evolution of the Central Catalan margin (North-western Mediterranean). Tectonophysics, 315, 209-229.

Roca, E., Guimerà J., 1992. The Neogene structure of the eastern Iberian margin: structural constraints on the crustal evolution of the València trough (Western Mediterranean). Tectonophysics, 203, 203-218.

Rodríguez, R., Blanco, A., 2012. Inquiry into the interactions between the Works on the Holy Family Temple and the construction of a high Speedy rail túnel between the Sants and La Sagrera stations in Barcelona. Revista de Obras Públicas, 3529, 7–30.

Sàbat, F., Roca, E., Muñoz, J.A., Vergés, J., Santanach, P., Sans, M., Masana, E., Estévez, A., Santisteban, C., 1997. Role of extension and compression in the evolution of the eastern margin of Iberia: Thde ESCI-Valencia Trough seismic profile. Revista Sociedad Geológica España, 8, 431-448.

Santanach, P., Casas, J. M.; Gratacós, O., Liesa, M., Muñoz, J.A., Sàbat, F. (2011). Variscan and Alpine structure of the hills of Barcelona: geology in an urban área. Journal of Iberian Geology, 37 (2), 121-136. doi: 10.5209/rev_JIGE.2011.v37.n2.2

Tambara, M., Nishigaki, M., Hashimoto, T., Shinshi, Y., Daito, K., 2003. Basic concept on preservation natural groundwater flows from intercepting by underground structure, in: Kono, Nishigaki and Komatsu (Eds.), Groundwater Engineering. Swets and Zeitlinger, Lisse, pp. 217-222.

The German Society for Geotechnics (DGGT), ed. 2012. Recommendations of the Committee for Waterfront Structures Harbours and Waterways, Eight Edition. Ernst & Sohn

Verlag für Architektur und technische Wissenschaften GmbH & Co. KG, Berlin, Germany. doi: 10.1002/9783433601419.

UPC, 2003. Code Visual Transin 1.1 R65. Developed in the Department of Geotechnical Engineering and Geosciences (ETCG), UPC.

Van Baars, S., 2011. Causes of major geotechnical disasters. In: Vogt, Schuppener, Straub and Braü (Eds.), ISGSR 2011. Bundesanstalt für Wasserbau, Germany.

Vázquez-Suñe, E., Sánchez-Vila, X., Carrera, J., Marizza, M., Arandes, R., Gutiérrez, L.A., 1997. Rising groundwater levels in Barcelona: evolution and effects on urban structures. In: Chilton et al. (ed.) Groundwater in the urban area: problems processes and management. 27th Cong. Int. Assoc. Hydrogeologists (IAH), 21–27 September 1997, Nottingham, pp 267–271.

Vázquez-Suñe, E., Sánchez-Vila, X., 1999a. Groundwater modeling in urban areas as a tool for local authorities management: Barcelona case study (Spain). In: Ellis B (ed.) Impacts of urban growth on surface water and groundwater quality. IAHS no.259, IAHS, Wallingford, UK, pp 65–73

Vázquez–Suñé, E., Sánchez–Vila, X., Carrera, J., 1999b. Gestión de las aguas subterráneas en zonas urbanas, conceptualización y modelación: aplicación a Barcelona (España), en Tineo, A. (ed.), Hidrología Subterránea: Tucumán, Argentina, Instituto Superior de Correlación Geológica, 153–160.

Vázquez-Suñe, E., Sánchez-Vila, X., Carrera, J., 2005. Introductory review of specific factors influencing urban groundwater, an emerging branch of hydrogeology, with reference to Barcelona, Spain. Hydrogeology Journal. 13, 522-533.

Velasco, V., Cabello, P., Vázquez-Suñé, E., López-Blanco, M., Ramos, E., Tobau, I., 2012. A sequence stratigraphic based geological model for constraining hydrogeological modeling in the urbanized area of the Quaternary Besòs delta (NW Mediterranean coast, Spain). Geologica acta, 10(4), 373-393.

Vicenzi, V., Gargini, A., Goldscheider, N., 2009. Using tracer tests and hydrological observations to evaluate effects of túnel drainage on groundwater and surface Waters in the Northern Apennines (Italy). Hydrogeology Journal. 17, 135-150.

Figure captions

Figure 1. Geographical location of the study site. The path of the HST tunnel and of the subway lines (L2 and L5) are displayed together with the location of the Padilla shaft (triangle). The section where the geological profile was made is also displayed in this figure (A-A').

Figure 2. Detailed geology of the Sagrada Familia area. The tunnel and the BPW can be observed together with the Basilica and its foundations.

Figure 3. Plan view (up) of the location of the Sagrada Familia. The figure shows the boreholes (black dots) employed to perform a detailed geological profile around the Sagrada Familia (shown below). Natural Gamma logs used to validate the geological profile are also displayed below. These were taken at the boreholes. A fault was identified close to Cartagena street. The high vertical heterogeneity described was useful to predict the impacts. The dashed black line indicate the layers made up by fine materials which separates hydraulically the upper layers from the lower layers.

Figure 4. Location of the piezometers around the Sagrada Familia. The tunnel (double black line) and the BPW (black dots) can also be observed. Piezometric contour lines from the numerical model of Barcelona are also displayed (grey lines). Numbers indicate the position of the head in m.a.s.l.

Figure 5. Historical head evolution in the proximities of Sagrada Familia. Numerical results (lines) are supported by historical data (dots) measured at different piezometers since 1950. These piezometers are not the same than the used to monitor the construction since the model has been verified with data of decades ago.

Figure 6. a) Behaviour of the flow through the piles of the BPW. Given the location of the no flow boundaries, each pile was regarded as a partial horizontal barrier. b) Behaviour of

the flow to cross the area affected by the tunnel. The tunnel was assumed as a partial vertical barrier. Dots indicate the theoretical (and ideal) groundwater level caused by the construction of the tunnel. Distances used for the predictions are included.

Figure 7. Hydraulic head variation of the piezometers located upgradient.

Figure 8. Hydraulic head variation of the piezometers located downgradient.

Figure 9. a) Location of the piles (P55, P56, P57 and P59) and the piezometers (PZ5 and PZ11). b) Hydraulic head evolution of the piezometers PZ5 and PZ11. The drops correlated with the construction of the piles.

Figure 10. Location of the monitoring points where the soil movements where measured. The soil movement evolutions were evaluated at different sections perpendicular to the tunnel (Sections A to E).

Figure 11. Soil movement evolution at three of sections of monitoring points perpendicular to the tunnel (Sections B, D and E in figure 10). Each pair of plots corresponds to one section. Above each pair: displacement variations between the arrival of the EPB at the Sagrada Familia and four months later. Long term movements can be observed in these plots. The data depicted by the arrow with number 3 is used to evaluate the long term movements. Below each pair: displacements occurred only when the tunnel was excavated under the Sagrada Familia. These plots are useful to observe the short term movements. Points 1 and 2 are the times when the short time movements were observed to evaluate the effects.

Figure 12. a) Monitoring points (HS15, HS16 and HS17) and piezometer (PZ20) used to observe the correlation between the hydraulic head oscillations and the variations in the soil during the passage of the EPB. b) Evolution of soil displacements at three monitoring points (lines with symbols) and groundwater oscillations (black line)

Figure 13. Soil movement distribution at several piezometers before and after the excavation of the tunnel a) Movements just before the passage of the tunnel under the Sagrada

Familia. b) Movements just after the passage under the Sagrada Familia. c), d), e) and f) represent the soil movements one, two, three and four months after the excavation of the tunnel under the Sagrada Familia. In the middle, a schematic plot with the ideal behaviour indicates the points in time to which each plan view corresponds.

Figure 14. Soil movement distribution caused by the barrier effect. Above, the schematic ideal behaviour it is shown. Below, the increases in movement between December 2010 and January 2011 are displayed in the left plain view while the increases between December and March 2011 are on the right. The plot with the ideal behaviour indicates the general position of the soil in these months.

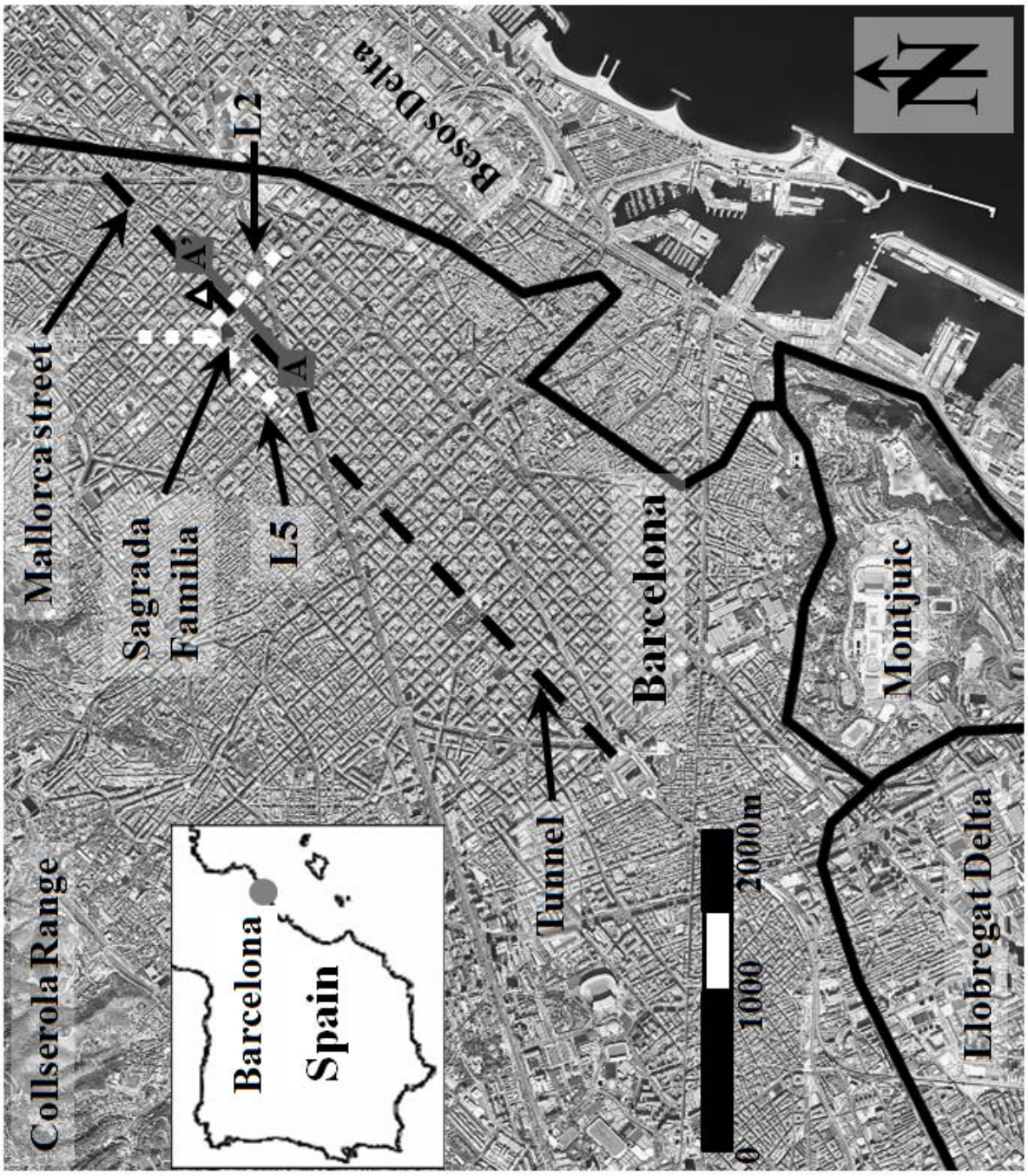
Collserola Range
Mallorca street
Sagrada Familia
A'
A
L2
L5
Besos Delta
Barceloma
Tunnel
Montjuic
Llobregat Delta
Barcelona
Spain
0
1000
2000m
N

Figure 1

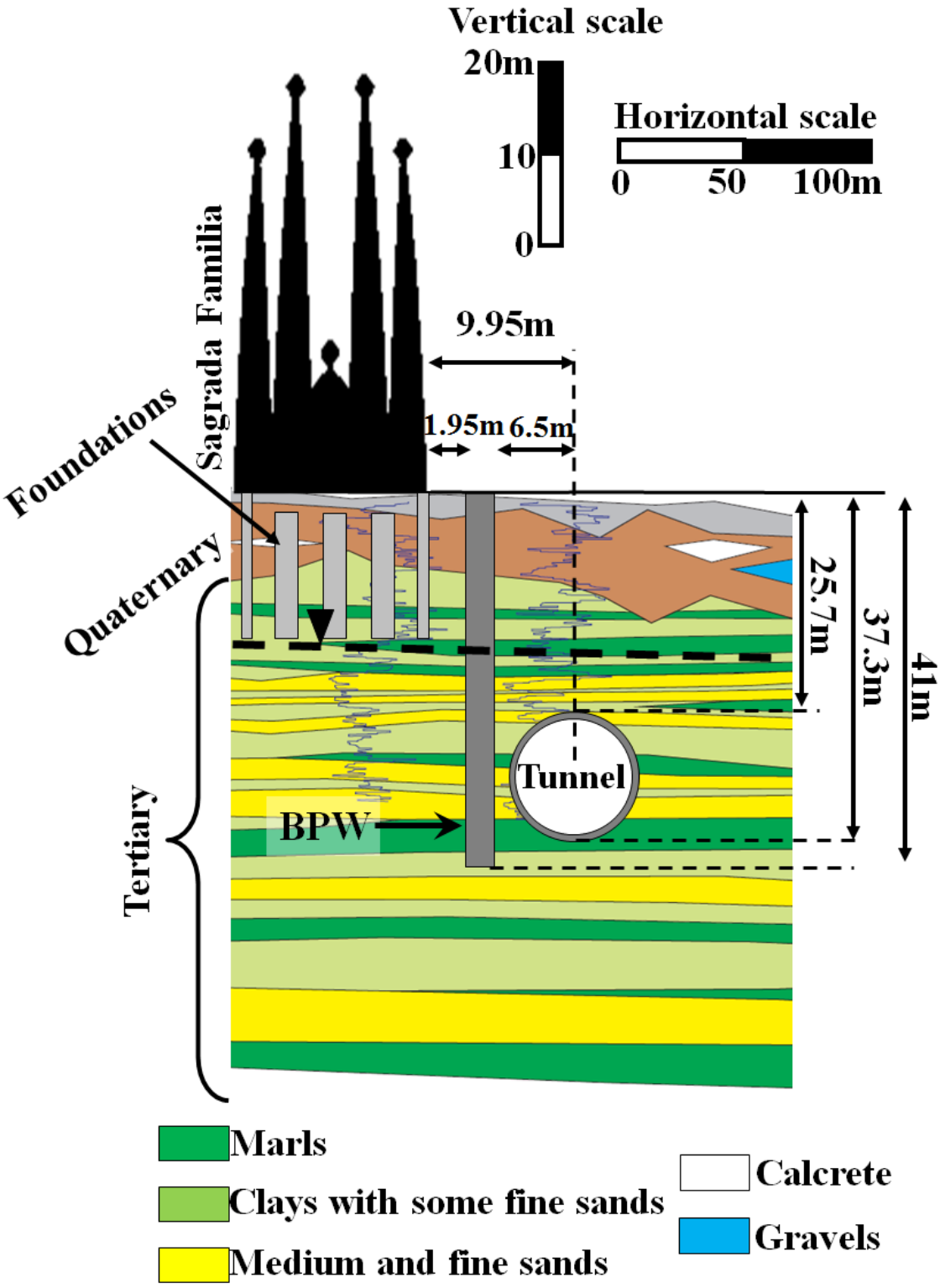
Vertical scale
20m
10
0
Horizontal scale
0
50
100m
Sagrada Familia
9.95m
1.95m
6.5m
Foundations
Quaternary
Tertiary
25.7m
37.3m
41m
Tunnel
BPW
Marls
Clays with some fine sands
Medium and fine sands
Calcrete
Gravels

Figure 2

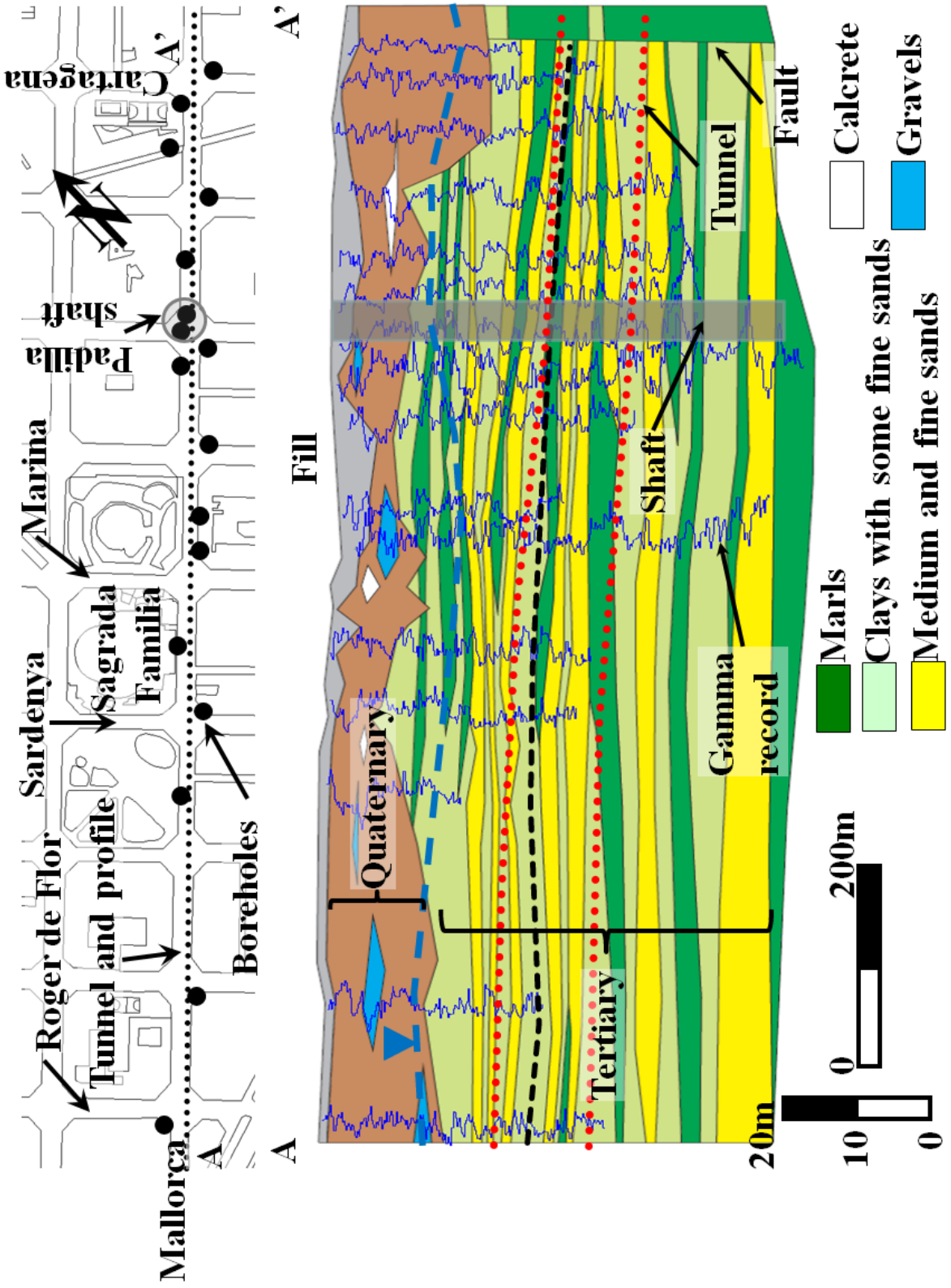
Mallorca
Roger de Flor
Sardenya
Marina
Padilla
shaft
Cartagena
A
A'
Tunnel and profile
Boreholes
Sagrada
Familia
A
A'
Fill
Quaternary
Tertiary
Shaft
Tunnel
Fault
Gamma
record
Calcrete
Gravels
Marls
Clays with some fine sands
Medium and fine sands
20m
10
0
0
200m

Figure 3

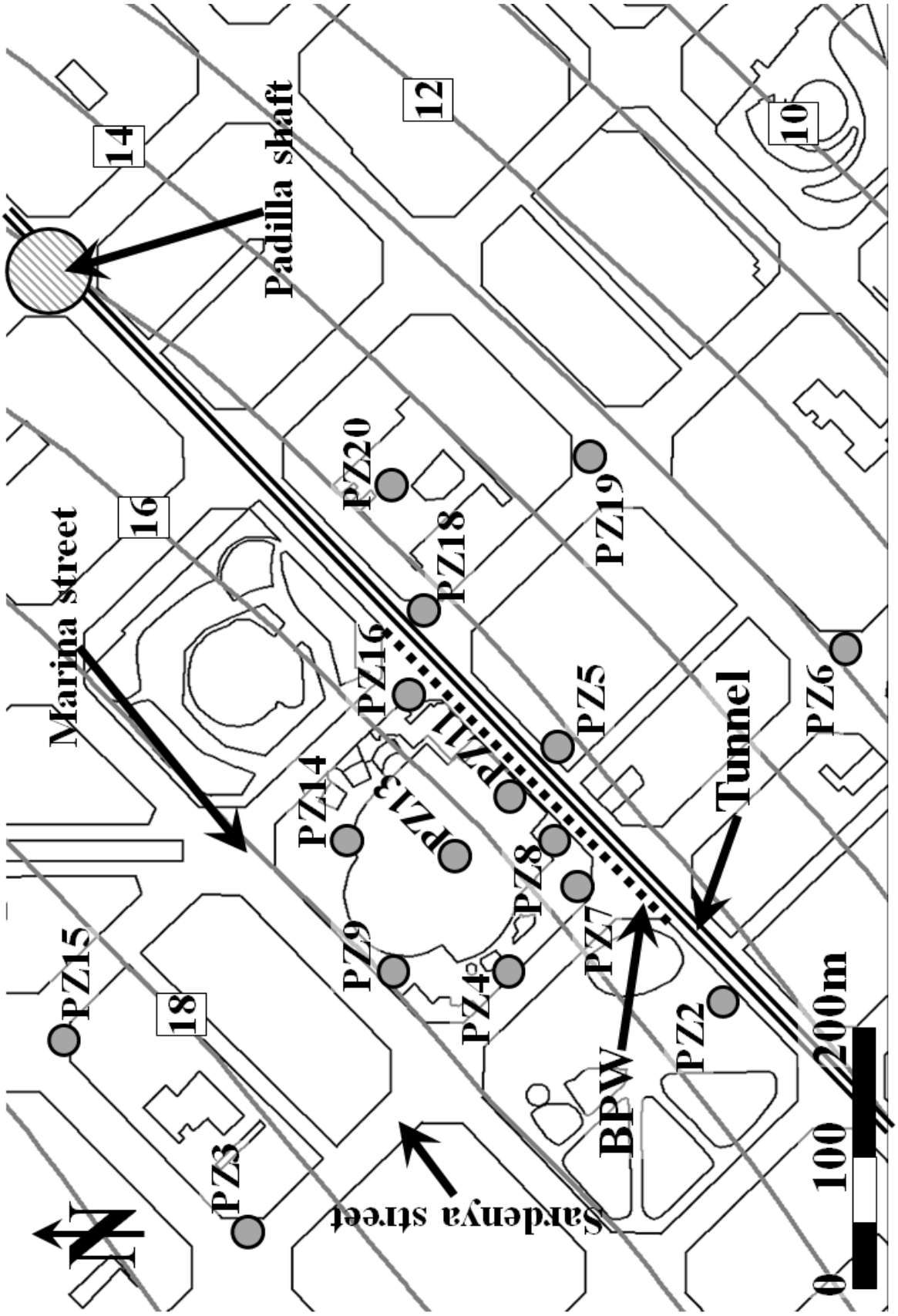
Padilla shaft
Marina street
Tunnel
Sardenya street
BPW
PZ20
PZ19
PZ18
PZ16
PZ14
PZ15
PZ3
PZ9
PZ4a
PZ8
PZ7
PZ2
PZ5
PZ6
OPZ11
OPZ13
12
14
16
18
10
0
100
200m
N

Figure 4

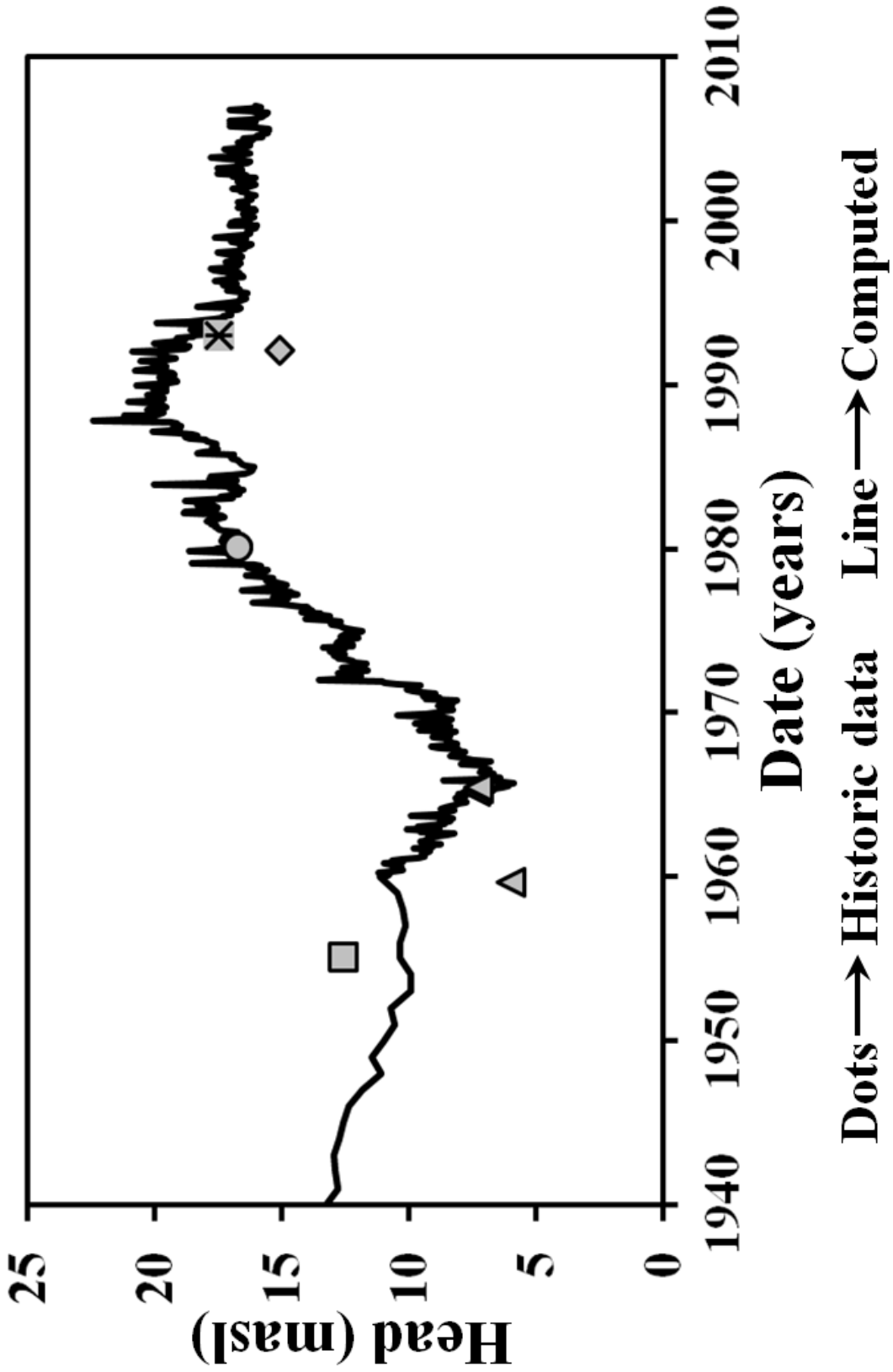
Head (masl)
25
20
15
10
5
0
1940
1950
1960
1970
1980
1990
2000
2010
Date (years)
Dots ⟶ Historic data Line ⟶ Computed

Figure 5

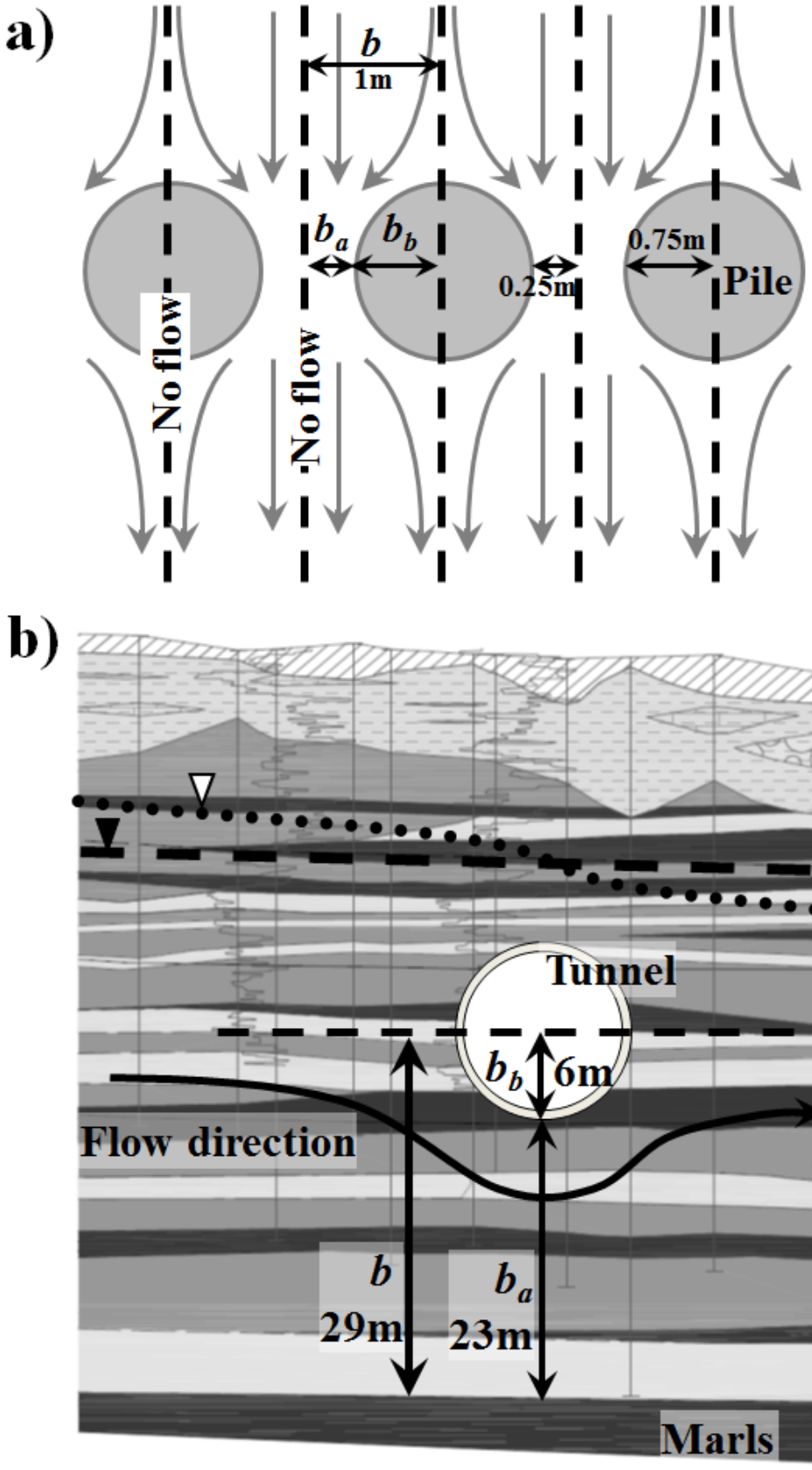
a)
b
1m
b_a
b_b
0.25m
0.75m
Pile
No flow
No flow
b)
Tunnel
b_b
6m
Flow direction
b
29m
b_a
23m
Marls

Figure 6

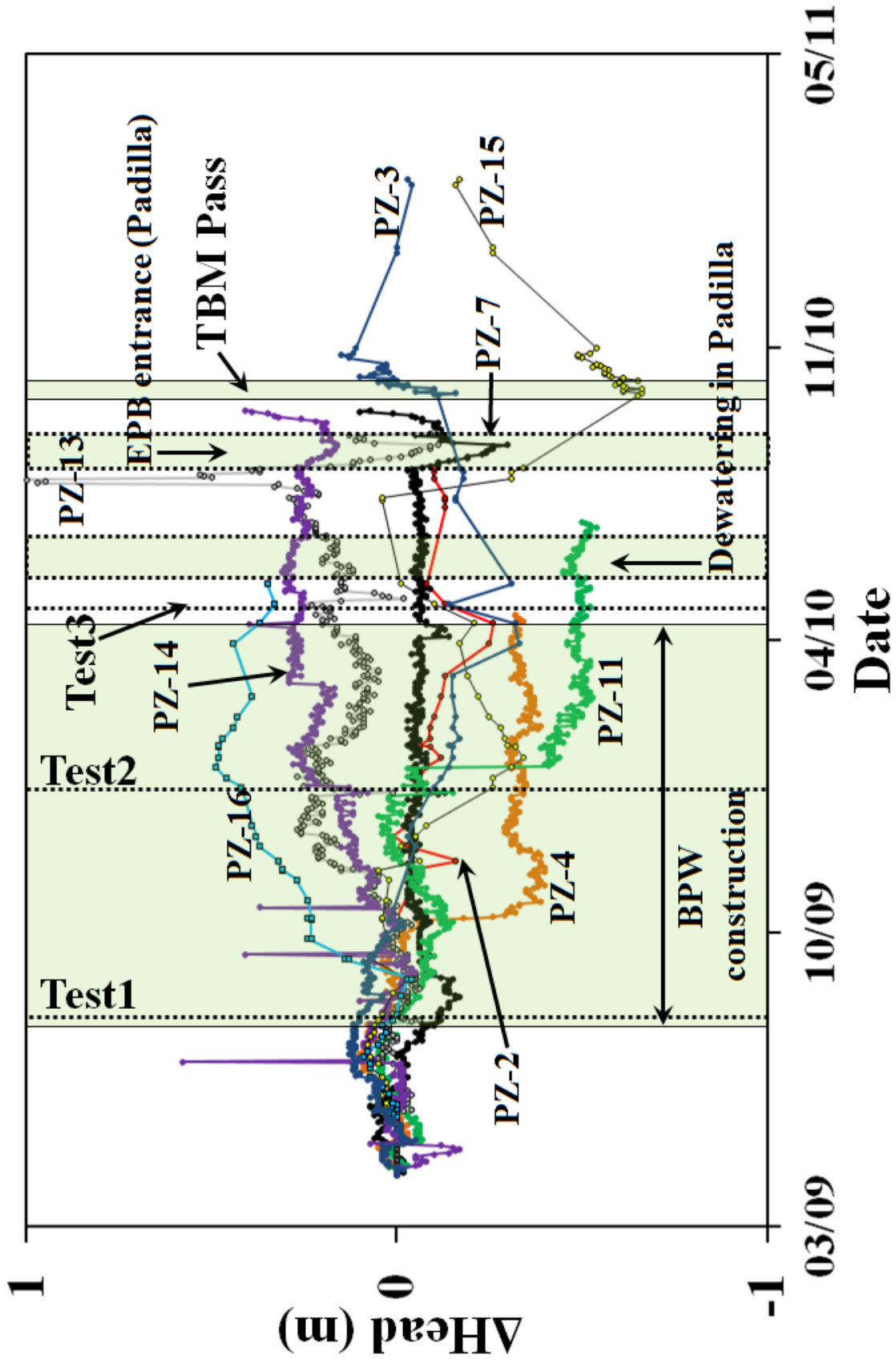
ΔHead (m)
1
0
-1
03/09
10/09
04/10
11/10
05/11
Date
EPB entrance (Padilla)
TBM Pass
Dewatering in Padilla
BPW construction
Test1
Test2
Test3
PZ-13
PZ-14
PZ-16
PZ-2
PZ-4
PZ-11
PZ-7
PZ-3
PZ-15

Figure 7

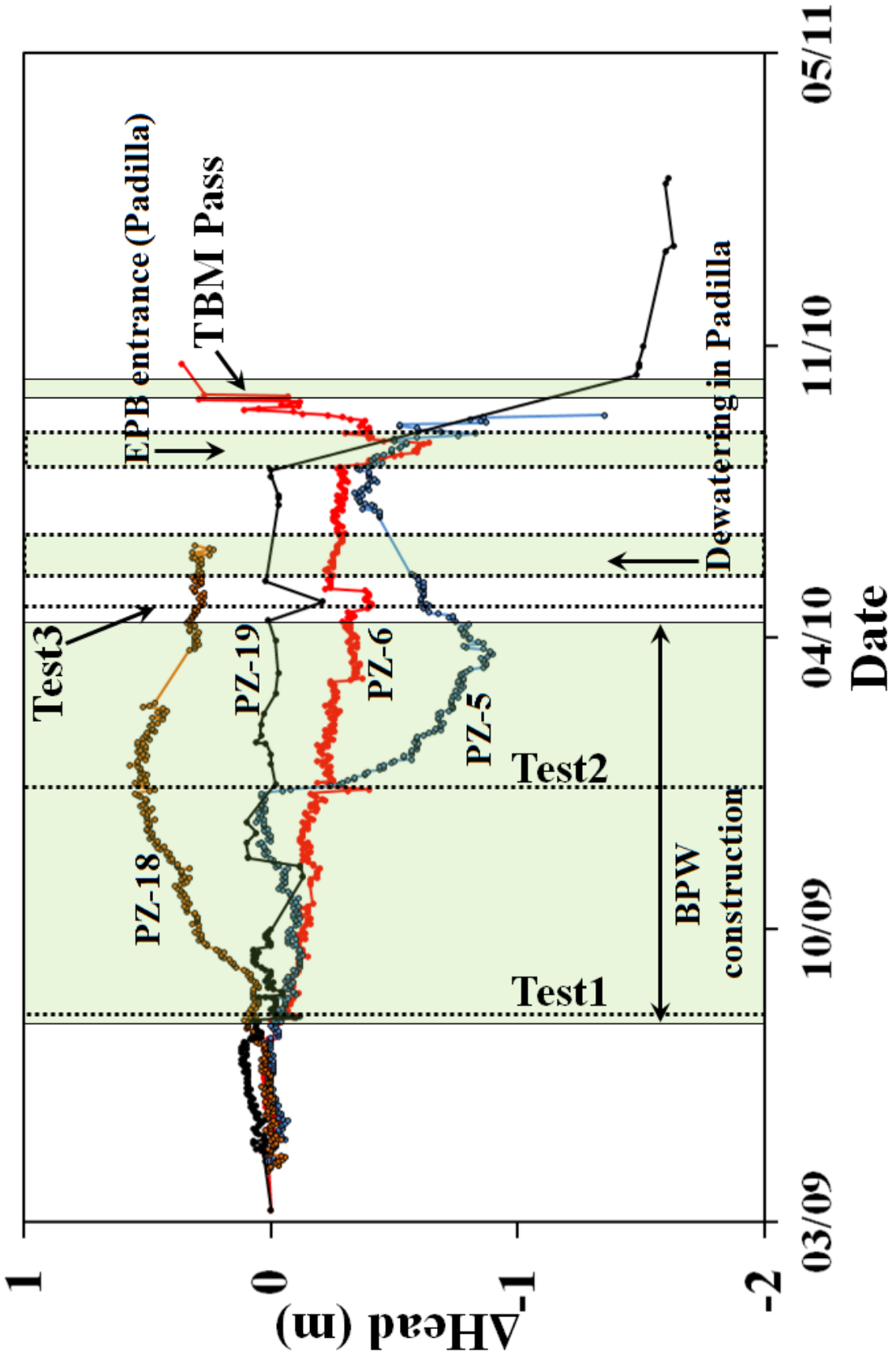
EPB entrance (Padilla)
TBM Pass
Dewatering in Padilla
Test3
PZ-19
PZ-6
PZ-5
PZ-18
Test2
Test1
BPW construction
ΔHead (m)
Date
1
0
-1
-2
03/09
10/09
04/10
11/10
05/11

Figure 8

a)
N
Sagrada
Familia
BPW
PZ-11
PZ-5
P59
P57
P56
P55
b)
BPW
construction
ΔHead (m)
0.5
0
-0.5
-1
-1.5
03/09
06/09
09/09
12/09
03/10
06/10
Date

Figure 9

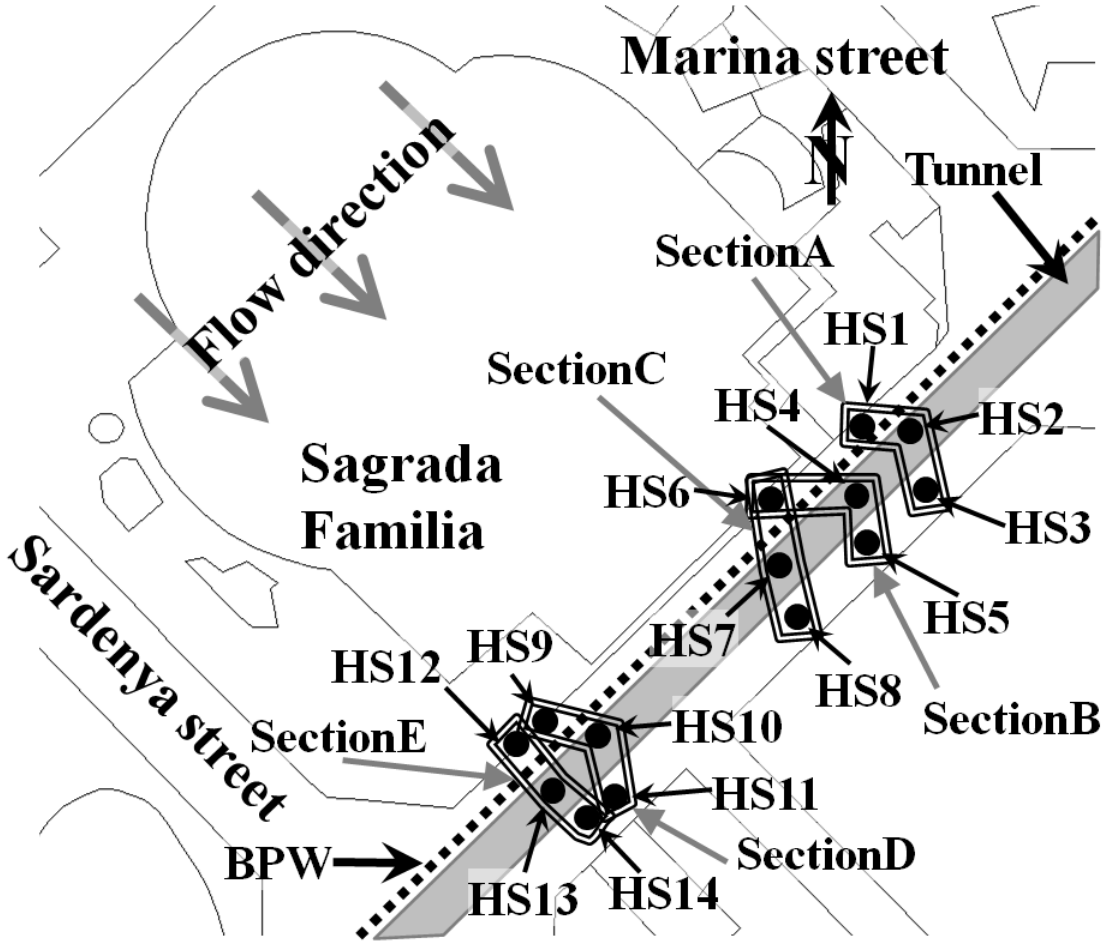
Marina street
N
Tunnel
Flow direction
SectionA
HS1
SectionC
HS4
HS2
Sagrada
Familia
HS6
HS3
HS5
HS7
HS9
HS12
HS8
SectionB
HS10
SectionE
HS11
SectionD
BPW
HS13
HS14
Sardenya street

Figure 10

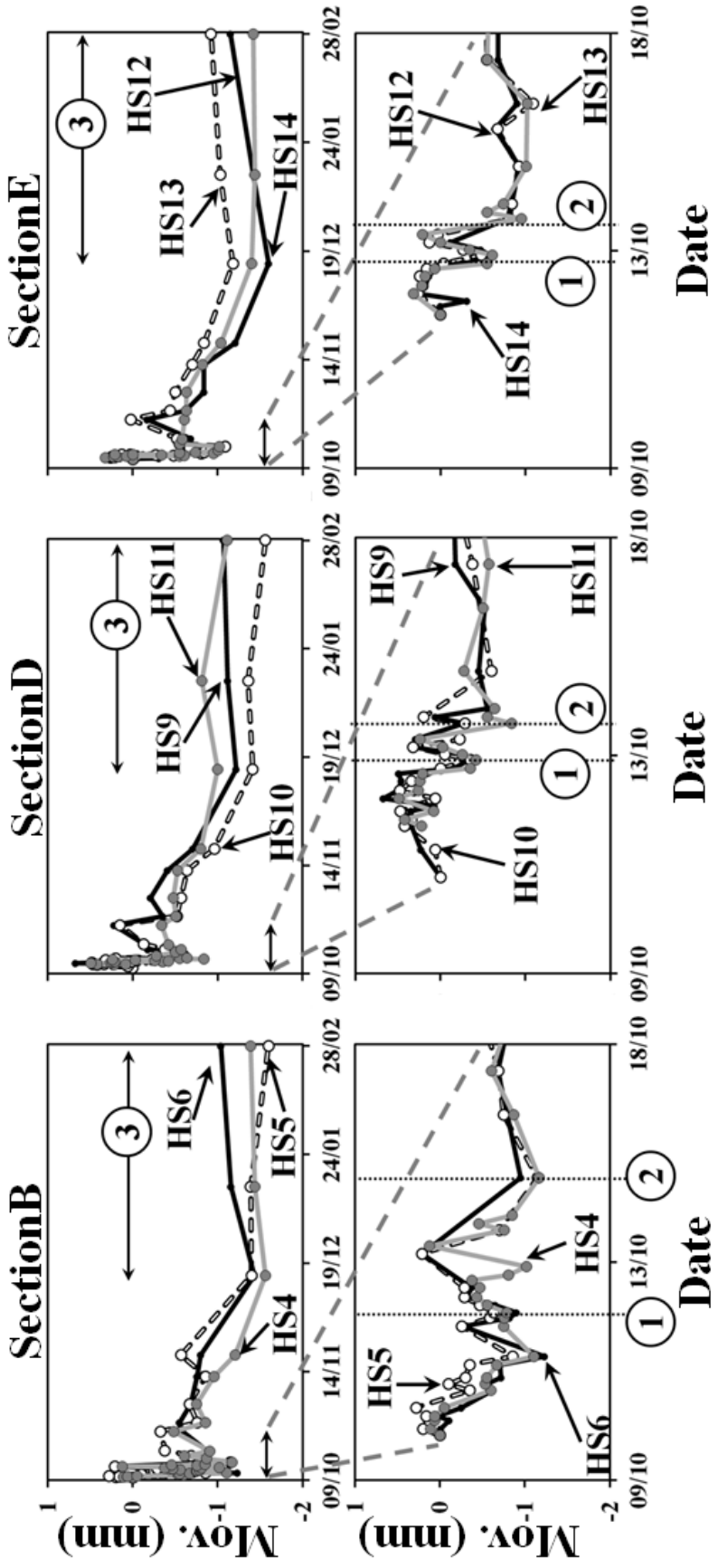
SectionB
SectionD
SectionE
Mov. (mm)
Date
09/10
14/11
19/12
24/01
28/02
13/10
18/10
HS4
HS5
HS6
HS9
HS10
HS11
HS12
HS13
HS14
1
2
3

Figure 11

a)
Sagrada Familia
BPW
Tunnel
HS17
HS15
HS16
PZ20
N
b)
Soil movement (mm)
1
0
-1
24/09/10
27/09/10
30/09/10
03/10/10
06/10/10
Date
PZ20 (Head)
HS15
HS16
HS17
Head (m.a.s.l.)
25
20
15
10

Figure 12

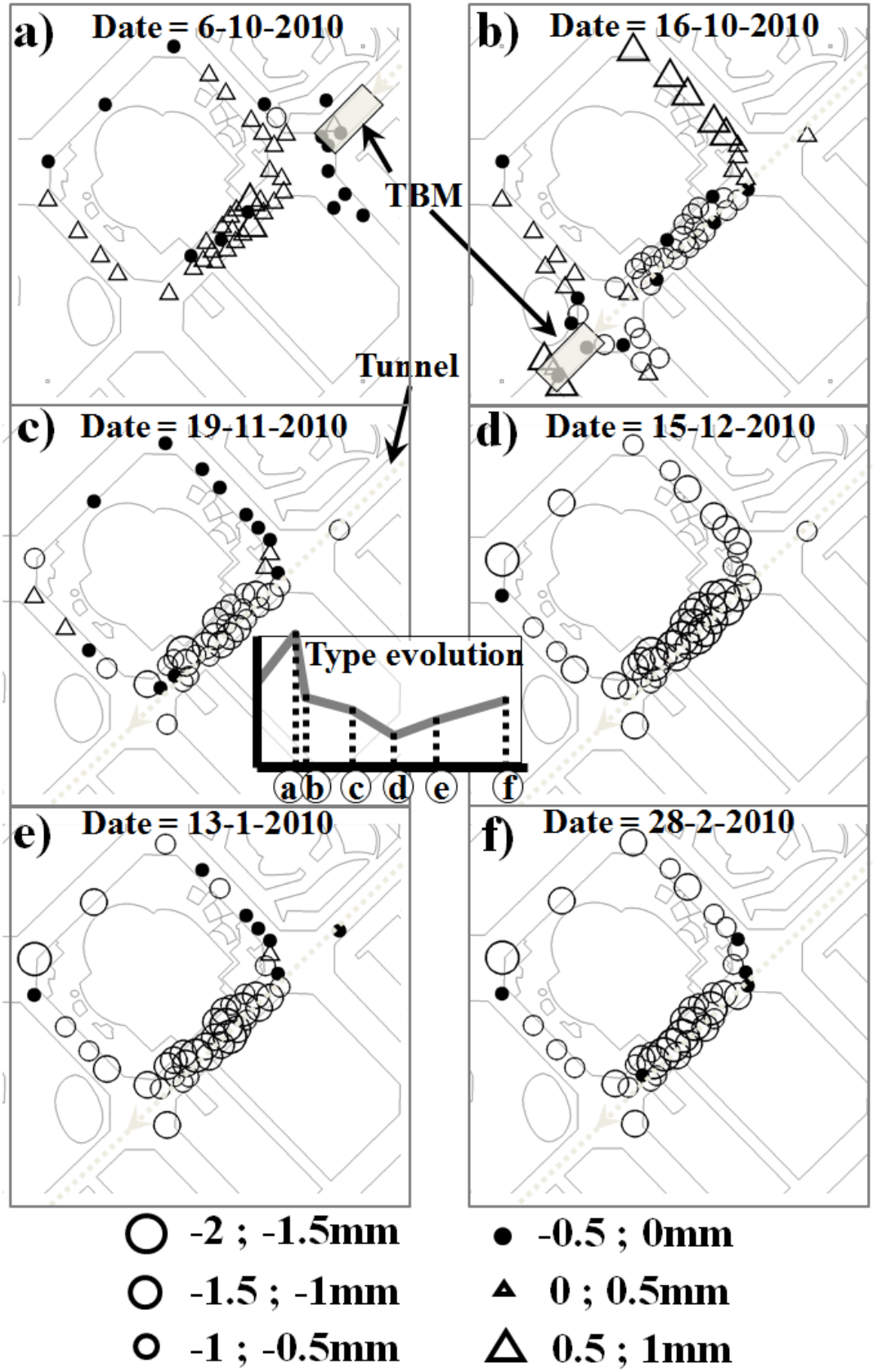
a) Date = 6-10-2010
b) Date = 16-10-2010
TBM
Tunnel
c) Date = 19-11-2010
d) Date = 15-12-2010
Type evolution
a b c d e f
e) Date = 13-1-2010
f) Date = 28-2-2010
-2 ; -1.5mm
-1.5 ; -1mm
-1 ; -0.5mm
-0.5 ; 0mm
0 ; 0.5mm
0.5 ; 1mm

Figure 13

Figure 14

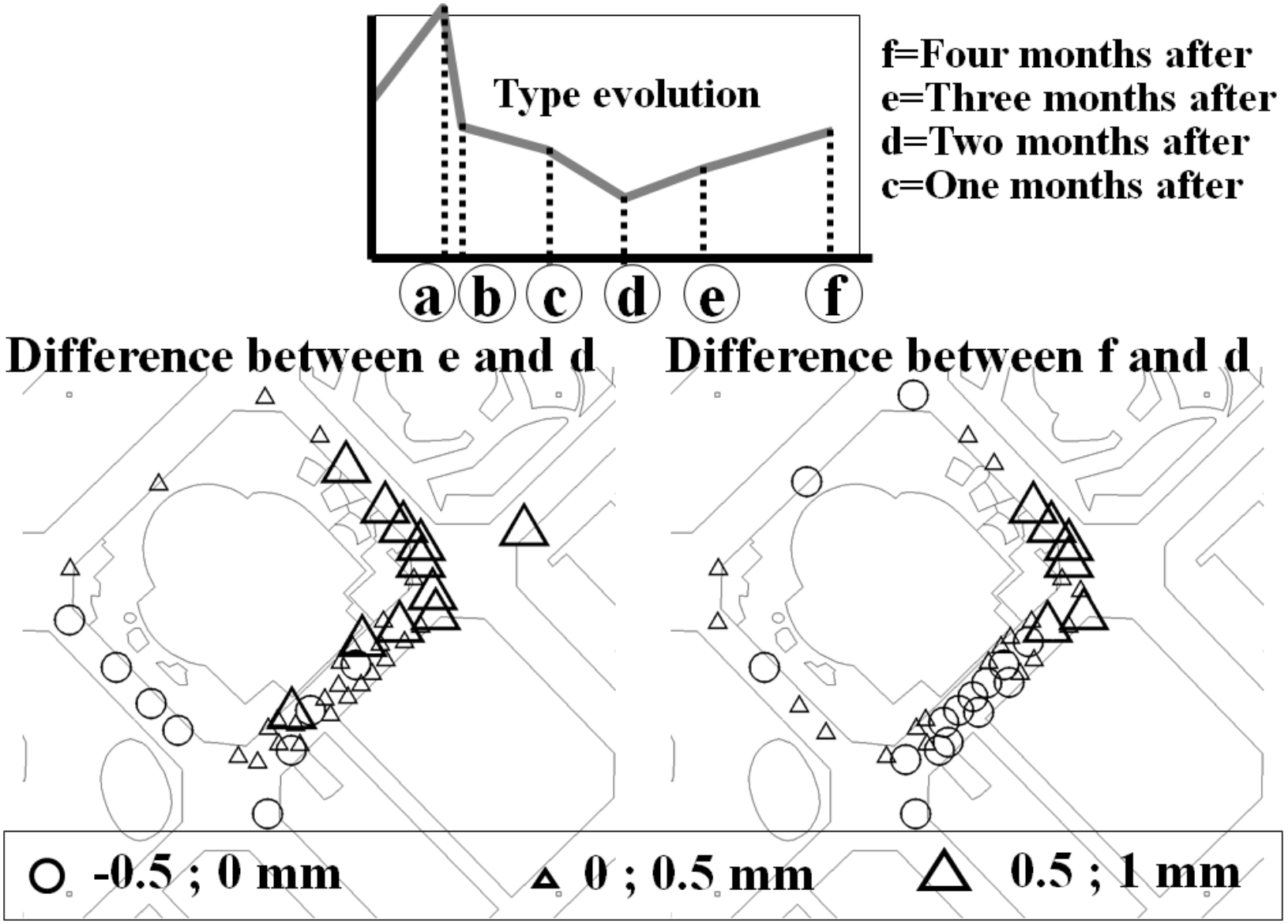
Type evolution
f=Four months after
e=Three months after
d=Two months after
c=One months after
a
b
c
d
e
f
Difference between e and d
Difference between f and d
-0.5 ; 0 mm
0 ; 0.5 mm
0.5 ; 1 mm

Table captions

Table 1. Characteristics of the piezometers located around the Sagrada Familia. Symbols located in the BPW column indicates the behaviour of the head at each piezometer due to the construction of the BPW. Piezometers of shaded cells are the screened in shallower layers (less than 30 m depth).

Table 2. Numerical and analytical predictions of the expected impacts (barrier effect and soil movements caused by the barrier effect).

Table 3. Summary of the observations at the monitoring points of the sections shown in Figure 10. Up, On and Down refer to the position of the monitoring points with respect to the tunnel and the flow direction (Up = Upgradient, On = Above the tunnel, and Down = Downgradient). Short term movements are Settlements 1 and 2, which correspond to the points 1 and 2 in the plots of the Figure 10. Long term movements are the movements caused by the barrier effect. The total movements attributable to the barrier effect are shown in the column on the right.

Table 1

Name	Initial head (masl)	BPW	Min. screen depth (m)	Max. screen depth (m)	Name	Initial head (masl)	BPW	Min. screen depth (m)	Max. screen depth (m)
PZ-2	**15.2**	↓	0	40	**PZ-13**	**14.0**	↑	0	25
PZ-3	**16.9**	↓	0	48	**PZ-14**	**14.6**	↑	0	29.5
PZ-4	**15.6**	↓	0	40	**PZ-15**	**18.0**	↓	0	45.8
PZ-5	**15.0**	↓	38	42	**PZ-16**	**13.0**	↑	0	23.5
PZ-6	**15.5**	↓	0	45.8	**PZ-18**	**13.0**	↑	0	35
PZ-7	**15.6**	=	0	48	**PZ-19**	**15.0**	=	0	37.5
PZ11	**15.7**	↓	31	37					

Table 2

Impact	Predictions			
	Structure	Numerical		Analytical
Barrier effect	Tunnel	Local	1.25 m	1.5 m
		Regional	0.5 m	0.2 m
	BPW	Local	-	0.06 m
		Regional	-	0.057 m
Soil movements	Tunnel	Local	0.54 mm	0.65 mm
		Regional	0.22 mm	0.08 mm
	BPW	Local	-	0.026 mm
		Regional	-	0.025 mm

Table 3

Section	Point	Settlement 1 (mm)	Settlement 2 (mm)	Movement S_B (mm)	Difference S_B (mm)
A	HS1 - Up	-0.92	-0.56	0.28	0.11
	HS2 - On	-0.72	-0.79	0.54	
	HS3 - Down	-1.03	-0.83	0.17	
B	HS6- Up	-1.23	-0.95	0.39	0.59
	HS4- On	-1.11	-1.17	0.17	
	HS5 - Down	-0.86	-1.15	-0.2	
C	HS6 - Up	-0.92	-0.95	0.39	0.72
	HS7 - On	-0.87	-1.22	-0.06	
	HS8 - Down	-0.81	-0.98	-0.33	
D	HS9 - Up	-0.34	-0.45	0.15	0.26
	HS10 - On	-0.34	-0.6	-0.15	
	HS11 - Down	-0.42	-0.28	-0.11	
E	HS12 -Up	-0.58	-0.79	0.45	0.47
	HS13 - On	-0.48	-0.81	0.26	
	HS14 - Down	-0.61	-0.95	-0.02	